Ultrasound in medicine and biology

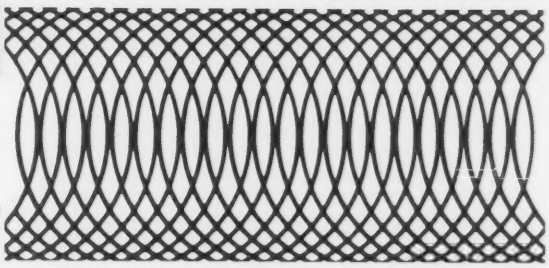

Author–Subject Index
Volume 24 (1998)

Compiled by

Michael Halliwell

Department of Medical Physics, Bristol General Hospital, Bristol BS1 6SY, United Kingdom

ELSEVIER

ELSEVIER

Ultrasound in Med. & Biol., Vol. 25, pp. 651–718, 1999
Copyright © 1999 World Federation for Ultrasound in Medicine & Biology
Printed in the USA. All rights reserved
0301-5629/99/$–see front matter

PII S0301-5629(99)00022-8

AUTHOR/SUBJECT INDEX

A

3D echocardiography
prognostic significance of color Doppler findings in head and neck tumors (Delorme), 1311

3D imaging
3-D colour Doppler image quantification of breast masses (Carson), 945
3-D sonographic volume measurement of the cerebral ventricular system: *in vitro* validation (Kampmann), 1169
analysis of linear, area and volume distortion in 3D ultrasound imaging (Tong), 355
3-D sonographic volume measurement of the cerebral ventricular system: *in vitro* validation (Kampmann), 1169
analysis of linear, area and volume distortion in 3D ultrasound imaging (Tong), 355
automatic registration of 3-D ultrasound images (Rohling), 841
automatic three-dimensional reconstruction and characterization of articular cartilage from high-resolution ultrasound acquisitions (Lefebvre), 1369
dynamic imaging of coronary stent structures: an ECG-gated three-dimensional intracoronary ultrasound study in humans (Bruining), 631
echo contrast-enhanced three-dimensional power Doppler of intracranial arteries (Postert), 953
estimation of the human liver volume and configuration using three-dimensional ultrasonography: effect of a high-caloric liquid meal (Hausken), 1357
in vitro evaluation of three-dimensional ultrasonography based on magnetic scanhead tracking (Gilja), 1161
influence of ECG-triggered data acquisition on reliability for carotid plaque volume measurements with a magnetic sensor three-dimensional ultrasound system (Delcker), 601
intra- and inter-observer variability and reliability of prostate volume measurement via two-dimensional and three-dimensional ultrasound imaging (Tong), 673
limitations for three-dimensional ultrasound imaging through a bore-hold trepanation (Suhm), 663
rapid calibration for 3-D freehand ultrasound (Prager), 855
three-dimensional ultrasound imaging (Nelson), 1243

A

Abraham, P., see Roy, E.
Acanfora, D., see Rengo, C.
Ackerstaff, R. G. A., see de Groot, E.
Ackerstaff, R. G. A., see Montauban van Swijndregt, A. D.

Acoustic anisotropy
kinetics of the "Black Hole" phenomenon in ultrasound backscattering measurements with red blood cell aggregation (Qin), 245

Acoustic bone windows
diagnosis and monitoring of middle cerebral artery occlusion with contrast-enhanced transcranial color-coded real-time sonography in patients with inadequate acoustic bone windows (Postert), 333

Acoustic injection
an acoustic injection test object for colour flow imaging systems (Li), 161

Acoustospectroscopy
quantitative ultrasonic analysis of liver metastases (Huisman), 67

Adnexal tumors
analysis of blood flow in adnexal tumors by using color Doppler imaging and pulsed spectral analysis (Takac), 1137

Ageing
assessment of carotid wall motion and stiffness with tissue Doppler imaging (Schmidt-Trucksäss), 639
blood-flow velocities and their relationships in carotid and middle cerebral arteries (Nagai), 1131
the development of hemodynamics in the extracranial carotid and vertebral arteries (Schöning), 655
ultrasonic and viscoelastic properties of skin under transverse mechanical stress *in vitro* (Pan), 995

Ahuja, A., see Chan, S.-T.
Ahuja, A., see Ying, M.
Alam, S. K. and Parker, K. J.: color flow mapping, 607 (Letter)
Alam, S. K. and Parker, K. J.: in response to K. Ferrara, 612 (Letter)
Albanese, S. A., see Spadaro, J. A.
Alcazar, J. L. and Laparte, C.: *in vivo* validation of the time domain velocity measurement technique of blood flow in human fetuses, 9
Alderman, J. L., see Brown, J. M.
Algra, A., see Simons, P. C. G.

Aliasing
aliasing-tolerant color Doppler quantification of regurgitant jets (Stewart), 881

Allard, L., see Qin, Z.
Alter, A., Rozenszajn, L. A., Miller, H. I. and Rosenschein, U.: ultrasound inhibits the adhesion and migration of smooth muscle cells in vitro, 711

Amniotic fluid volume
fetal biometry and outcome in monochorionic vs. dichorionic twin pregnancies; a retrospective cross-sectional matched-control study (Snijder), 197

Anderson, T., see Li, S. F.
Anderson, T., see Moran, C. M.

Angiogenesis
3-D colour Doppler image quantification of breast masses (Carson), 945
analysis of blood flow in adnexal tumors by using color Doppler imaging and pulsed spectral analysis (Takac), 1137

atlas of ultrasound and ductal echography of the breast (Fonda), 925

Anthony, P., Chandraratna, N., Gallet, J., Jones, J. P., Do, Y., Gunawardana, R. and Narang, Y.: an investigation of possible effects of high-frequency ultrasound on cellular integrity of cultured fibroblasts, 911

Aorta
acoustic properties of atherosclerosis of human aorta obtained with high-frequency ultrasound (Saijo), 1061
ultrasound inhibits the adhesion and migration of smooth muscle cells *in vitro* (Alter), 711

Arefiev, A., Prat, F., Chapelon, J. Y., Tavakkoli, J. and Cathignol, D.: ultrasound-induced tissue ablation: studies on isolated, perfused porcine liver, 1033

Aristizábal, O., Christopher, D. A., Foster, F. S. and Turnbull, D. H.: 40-MHz echocardiography scanner for cardiovascular assessment of mouse embryos, 1407

Artefacts
artifacts in intravascular ultrasound imaging during coronary artery stent implantation (Finet), 793
limits on the contrast of strain concentrations in elastography (Kallel), 1215

Arterial stiffness
assessment of carotid wall motion and stiffness with tissue Doppler imaging (Schmidt-Trucksäss), 639
effect of timing of blood pressure measurement in the assessment of arterial stiffness: The SMART Study (Simons), 1285

Arteries
a brief history of Doppler ultrasound in the diagnosis of peripheral vascular disease (Sigel), 169
a new 1-MHz probe for transcranial Doppler sonography in patients with inadequate temporal bone windows (Klötzsch), 101
a noninvasive method to estimate pulse wave velocity in arteries locally by means of ultrasound (Brands), 1325
acoustic properties of atherosclerosis of human aorta obtained with high-frequency ultrasound (Saijo), 1061
artifacts in intravascular ultrasound imaging during coronary artery stent implantation (Finet), 793
assessment of carotid wall motion and stiffness with tissue Doppler imaging (Schmidt-Trucksäss), 639
automated intima-media thickness: The Los Angeles Atherosclerosis Study (Dwyer), 981
bladder filling reduces femoral artery wall distension and strain: beware of a full bladder! (Willekes), 803
blood-flow velocities and their relationships in carotid and middle cerebral arteries (Nagai), 1131
diagnosis and monitoring of middle cerebral artery occlusion with contrast-enhanced transcranial color-coded real-time sonography in patients with inadequate acoustic bone windows (Postert), 333
echo contrast-enhanced three-dimensional power Doppler of intracranial arteries (Postert), 953
effect of timing of blood pressure measurement in the assessment of arterial stiffness: The SMART Study (Simons), 1285

in vivo validation of the time domain velocity measurement technique of blood flow in human fetuses (Alcázar), 9
intravascular ultrasound elastography in human arteries: initial experience *in vitro* (de Korte), 401
quantification of iliac artery stenoses: a methodological comparative study between intravascular ultrasound, arteriography and duplex scanning (Vogt), 963
reliability and reproducibility of automated contour analysis in intravascular ultrasound images of femoropopliteal arteries (van der Lugt), 43
the development of hemodynamics in the extracranial carotid and vertebral arteries (Schöning), 655
the use of intravascular ultrasound for intraoperative assessment during semiclosed thromboendarterectomy (Vogt), 21
ultrasonic tissue characterization for coronary care unit patients with acute myocardial infarction (Lin), 187
ultrasound imaging for arterial wall thickness measurement: an *in vitro* study with stereomicroscopic correlation (Raninen), 833
umbilical artery waveform analysis based on maximum, mean and mode velocity in early human pregnancy (Ursem), 1
variance components analysis of carotid and femoral intima-media thickness measurements (de Groot), 825

Artery wall
automated intima-media thickness: The Los Angeles Atherosclerosis Study (Dwyer), 981
bladder filling reduces femoral artery wall distension and strain: beware of a full bladder! (Willekes), 803
ultrasound imaging for arterial wall thickness measurement: an *in vitro* study with stereomicroscopic correlation (Raninen), 833
variance components analysis of carotid and femoral intima-media thickness measurements (de Groot), 825

Atherosclerosis
a brief history of Doppler ultrasound in the diagnosis of peripheral vascular disease (Sigel), 169
acoustic properties of atherosclerosis of human aorta obtained with high-frequency ultrasound (Saijo), 1061
assessment of carotid wall motion and stiffness with tissue Doppler imaging (Schmidt-Trucksäss), 639
effect of timing of blood pressure measurement in the assessment of arterial stiffness: The SMART Study (Simons), 1285
influence of ECG-triggered data acquisition on reliability for carotid plaque volume measurements with a magnetic sensor three-dimensional ultrasound system (Delcker), 601
quantification of iliac artery stenoses: a methodological comparative study between intravascular ultrasound, arteriography and duplex scanning (Vogt), 963
reliability and reproducibility of automated contour analysis in intravascular ultrasound images of femoropopliteal arteries (van der Lugt), 43
the use of intravascular ultrasound for intraoperative assessment during semiclosed thromboendarterectomy (Vogt), 21
ultrasonographic characterization of carotid plaques (Montauban van Swijndregt), 489

variance components analysis of carotid and femoral intima-media thickness measurements (de Groot), 825

Attenuation coefficient
acoustic properties of atherosclerosis of human aorta obtained with high-frequency ultrasound (Saijo), 1061
experimental study of stability of a contrast agent in an ultrasound field (Wu), 257
high frequency ultrasound properties of multicellular spheroids during heating (Gertner), 461
quantitative ultrasonic analysis of liver metastases (Huisman), 67
ultrasonic and viscoelastic properties of skin under transverse mechanical stress *in vitro* (Pan), 995

Auriol, F., see Diridollou, S.

Automated detection
the narrow band hypothesis: an interesting approach for high-intensity transient signals (HITS) detection (Roy), 375

Automated image analysis
automated intima-media thickness: The Los Angeles Atherosclerosis Study (Dwyer), 981
automatic three-dimensional reconstruction and characterization of articular cartilage from high-resolution ultrasound acquisitions (Lefebvre), 1369
beat averaging alternatives for transmitral Doppler flow velocity images (Hall), 971
evaluation of model-based processing algorithms for averaged transmitral spectral Doppler images (Hall), 55
quantification of sonographic echogenicity with grey-level histogram width: a clinical tissue characterization (Maeda), 225
reliability and reproducibility of automated contour analysis in intravascular ultrasound images of femoropopliteal arteries (van der Lugt), 43
variance components analysis of carotid and femoral intima-media thickness measurements (de Groot), 825

B

Büttner, T., see Postert, T.

B/A
measurements of the nonlinearity parameter B/A of contrast agents (Wu), 153

Bachtold, M. R., Rinaldi, P. C., Jones, J. P., Reines, F. and Price, L. R.: focused ultrasound modifications of neural circuit activity in a mammalian brain, 557

Backscatter
acoustic modeling of shell-encapsulated gas bubbles (Frinking), 523
assessment of bone density using ultrasonic backscatter (Wear), 689
comparison of the Rayleigh and K-distribution models using *in vivo* breast and liver tissue (Molthen), 93
dissolution of multicomponent microbubbles in the bloodstream: 1. Theory (Kabalnov), 739

dissolution of multicomponent microbubbles in the bloodstream: 2. Experiment (Kabalnov), 751
effects of a sudden flow reduction on red blood cell rouleau formation and orientation using RF backscattered power (Qin), 503
evaluation of acoustical parameter sensitivity to age-related and osteoarthritic changes in articular cartilage using 50-MHZ ultrasound (Chérin), 341
high frequency ultrasound properties of multicellular spheroids during heating (Gertner), 461
in vitro investigation of lymph node metastasis of colorectal cancer using ultrasonic spectral parameters (Noritomi), 235
kinetics of the "Black Hole" phenomenon in ultrasound backscattering measurements with red blood cell aggregation (Qin), 245
liquid or solid ultrasonically tissue-mimicking materials with very low scatter (Madsen), 535
onset delay of acoustic second harmonic backscatter from bubbles or microspheres (Zheng), 513
quantification of the enhanced backscatter phenomenon from an intravenous and an intra-arterial contrast agent (Moran), 871
quantitative ultrasonic analysis of liver metastases (Huisman), 67
the value of thyroid parenchymal echogenicity as an indicator of pathology using the sternomastoid muscle for comparison (Ying), 1097
ultrasonic and viscoelastic properties of skin under transverse mechanical stress *in vitro* (Pan), 995
ultrasonic tissue characterization for coronary care unit patients with acute myocardial infarction (Lin), 187
ultrasound echogenicity in experimental venous thrombosis (Fowlkes), 1175
using phase information in ultrasonic backscatter for *in vivo* liver analysis (Molthen), 79

Bailey, M., see Vaezy, S.
Bakker, J., Olree, M., Kaatee, R., de Lange, E. E. and Beek, F. J. A.: *in vitro* measurement of kidney size: comparison of ultrasonography and MRI, 683
Barned, S., see Doida, Y.
Barnett, S. B., see Horder, M. M.
Baudry, M., see Roy, E.
Beach, K. W., see Jong, J.-M.
Beaune, J., see Finet, G.
Beek, F. J. A., see Bakker, J.
Bell, P. R. F., see Smith, J. L.
Bellotti, M., see Pennati, G.
Bendl, R., see Suhm, N.
Berdeaux, A, see Pellerin, D.
Bergelin, R. O., see Jong, J.-M.
Berger, G., see Chérin, E.
Berger, G., see Lefebvre, F.
Berkowitz, H. D., see Lee, D. J.
Berlit, P., see Klötzsch, C.
Berman, L., see Prager, R. W.
Berman, L., see Rohling, R. N.
Bernardes, J., see Bernardino, F.
Bernardino, F., Cardoso, R., Montenegro, N., Bernardes, J. and Marques de

Sa, J.: semiautomated ultrasonographic measurement of fetal nuchal translucency using a computer software tool, 51
Berson, M., see Diridollou, S.

Bioeffects
an investigation of possible effects of high-frequency ultrasound on cellular integrity of cultured fibroblasts (Chandraratna), 911
application of low-intensity ultrasound to growing bone in rats (Spadaro), 567
artificial cavitation nuclei significantly enhance acoustically induced cell transfection (Greenleaf), 587
effect of acoustic cavitation on platelets in the presence of an echo-contrast agent (Everbach), 129
defects generated in human stratum corneum specimens by ultrasound (Wu), 705
demonstration of potential noninvasive ultrasound brain therapy through an intact skull (Hynynen), 275
design and preliminary results of an ultrasound applicator for interstitial thermal coagulation (Lafon), 113
effects of pulsed ultrasound on embryonic development: an *in vitro* study (Ramnarine), 575
enhancement of ultrasonically-induced hemolysis by perfluorocarbon-based compared to air-based echo-contrast agents (Miller), 285
focused ultrasound modifications of neural circuit activity in a mammalian brain (Bachtold), 557
gas-body-based contrast agent enhances vascular bioeffects of 1.09 MHz ultrasound on mouse intestine (Miller), 1201
hemostasis of punctured blood vessels using high-intensity focused ultrasound (Vaezy), 903
in vivo heating of the guinea-pig fetal brain by pulsed ultrasound and estimates of thermal index (Horder), 1467
innovative technology for tissue disruption by explosive-induced shock waves (Kodama), 1459
sonochemicals increase the mutation frequency of V79 cells *in vitro* (Doida), 1209
temperature rise generated by ultrasound in the presence of contrast agent (Wu), 267
the interaction of ultrasonic heating and cavitation in vascular bioeffects on mouse intestine (Miller), 123
treatment of implanted liver tumors with focused ultrasound (Chen), 1475
ultrasound imaging of thermal therapy in *in vitro* liver (Gertner), 1023
ultrasound inhibits the adhesion and migration of smooth muscle cells *in vitro* (Alter), 711
ultrasound-induced temperature increase in guinea-pig fetal brain *in utero*: third-trimester gestation (Horder), 1501
ultrasound-induced temperature increase in the guinea-pig fetal brain *in vitro* (Horder), 697
ultrasound-induced tissue ablation: studies on isolated, perfused porcine liver (Arefiev), 1033

Biorheology
effects of a sudden flow reduction on red blood cell rouleau formation and orientation using RF backscattered power (Qin), 503

kinetics of the "Black Hole" phenomenon in ultrasound backscattering measurements with red blood cell aggregation (Qin), 245

Black hole
kinetics of the "Black Hole" phenomenon in ultrasound backscattering measurements with red blood cell aggregation (Qin), 245

Black, D., see Diridollou, S.

Bladder
bladder filling reduces femoral artery wall distension and strain: beware of a full bladder! (Willekes), 803
intraobserver and interobserver variance in the measurement of ultrasound-estimated bladder weight (Naya), 771

Bladder weight
intraobserver and interobserver variance in the measurement of ultrasound-estimated bladder weight (Naya), 771

Blood
dissolution of multicomponent microbubbles in the bloodstream: 1. Theory (Kabalnov), 739
dissolution of multicomponent microbubbles in the bloodstream: 2. Experiment (Kabalnov), 751

Blood flow
3-D colour Doppler image quantification of breast masses (Carson), 945
a brief history of Doppler ultrasound in the diagnosis of peripheral vascular disease (Sigel), 169
a new 1-MHz probe for transcranial Doppler sonography in patients with inadequate temporal bone windows (Klötzsch), 101
alteration of thyroid blood flow during the normal menstrual cycle in healthy Chinese women (Chan), 15
analysis of blood flow in adnexal tumors by using color Doppler imaging and pulsed spectral analysis (Takac), 1137
blood flow imaging and volume flow quantitation with intravascular ultrasound (Li), 203
blood flow through the ductus venosus in human fetus: calculation using Doppler velocimetry and computational findings (Pennati), 477
blood velocity profile in the ductus venosus inlet expressed by the mean/maximum velocity ratio (Kiserud), 1301
blood-flow velocities and their relationships in carotid and middle cerebral arteries (Nagai), 1131
color Doppler sonography of normal breasts: detectability of arterial blood vessels and typical flow patterns (Rettenbacher), 1307
duodenal meal stimulation leads to coeliac artery vasoconstriction and superior mesenteric artery vasodilatation: an intra-abdominal ultrasound study (Geelkerken), 1351
effects of a sudden flow reduction on red blood cell rouleau formation and orientation using RF backscattered power (Qin), 503
Gosling's Doppler pulsatility index revisited (Michel), 597
in vivo validation of the time domain velocity measurement technique of blood flow in human fetuses (Alcázar), 9
kinetics of the "Black Hole" phenomenon in ultrasound backscattering measurements with red blood cell aggregation (Qin), 245

lower extremity volumetric arterial blood flow in normal subjects (Holland), 1079
portal vein pulsatility ratio provides a measure of right heart function in chronic heart failure (Rengo), 327
the development of hemodynamics in the extracranial carotid and vertebral arteries (Schöning), 655
the narrow band hypothesis: an interesting approach for high-intensity transient signals (HITS) detection (Roy), 375
ultrasonic mapping of the microvasculature: signal alignment (Zagar), 809
umbilical artery waveform analysis based on maximum, mean and mode velocity in early human pregnancy (Ursem), 1

Blood mimicking
validation of a new blood-mimicking fluid for use in Doppler flow test objects (Ramnarine), 451

Blood pressure
effect of timing of blood pressure measurement in the assessment of arterial stiffness: The SMART Study (Simons), 1285

Blood vessel surgery
hemostasis of punctured blood vessels using high-intensity focused ultrasound (Vaezy), 903

Bolander, M. E., see Greenleaf, W. J.
Bolson, E. L., see Hausken, T.
Bom, N., see de Groot, E.
Bom, N., see Li, W.
Bond, A. D. and Preston, R. C.: the NPL Doppler fetal heart beat detector test facility, 443

Bone
application of low-intensity ultrasound to growing bone in rats (Spadaro), 567
assessment of bone density using ultrasonic backscatter (Wear), 689

Bone density
assessment of bone density using ultrasonic backscatter (Wear), 689

Bone growth
application of low-intensity ultrasound to growing bone in rats (Spadaro), 567

Book Reviews
a practical guide to ultrasound in obstetrics and gynecology. Eds. Sauerbrei, Nguyen and Nolan. (Smith), 1069
advances in echo imaging using contrast enhancement. Eds. Nanda, Schief and Goldberg. (Senior), 1511
atlas of ultrasound and ductal echography of the breast. Teboul and Halliwell. (Fonda), 925
atlas of ultrasound colour flow imaging. Ed. Goldberg. (Twining), 1514
clinical transesophageal echocardiography - a problem-oriented approach. Eds. Oka and Konstadt. (Wright), 307
diagnostic ultrasound - a logical approach. McGraham and Goldberg. (Bradley), 925

diagnostic ultrasound – principles and instruments (5th Edition) Kremkau. (Hoskins), 1221
intravascular ultrasound imaging in cronary artery disease. Ed. Siegel. (van der Steen), 1511
introduction to ultrasound. Eds Zweibel and Sohaey. (Duggan), 926
post-graduate course in vascular Doppler: a comprehensive course on videotapes Eds. Bolondi and Gaiani. (Duck), 613
safety of diagnostic ultrasound. Eds. Barnett and Kossoff. (Starritt), 1513
ultrasound contrast agents. Ed. Goldberg. (Perkins), 307

Boragk, R., see Schmidt-Trucksäss, A.
Bots, M. L., see Simons, P. C. G.
Bouzakaz, A., de Jong, N. and Cachard, C.: standard properties of ultrasound contrast agents, 469
Box, G., see Chen, L.
Bozzo, M., see Pennati, G.
Bradley, J., see Kabalnov, A.
Bradley, M. J.
Bradley, M. J.: diagnostic ultrasound - a logical approach, 925

Brain
3-D sonographic volume measurement of the cerebral ventricular system: *in vitro* validation (Kampmann), 1169
focused ultrasound modifications of neural circuit activity in a mammalian brain (Bachtold), 557

Brands, P. J., see Ledoux, L. A. F.
Brands, P. J., Willigers, J. M., Ledoux, L. A. F., Reneman, R. S. and Hoeks, A. P. G.: a noninvasive method to estimate pulse wave velocity in arteries locally by means of ultrasound, 1325
Brasseur, J. G., see Wu, S. J.
Braun, B., see Postert, T.
Braun, B., see Postert, T.
Brayman, A. A., see Doida, Y.

Breast
3-D colour Doppler image quantification of breast masses (Carson), 945
atlas of ultrasound and ductal echography of the breast (Fonda), 925
color Doppler sonography of normal breasts: detectability of arterial blood vessels and typical flow patterns (Rettenbacher), 1307
in vitro diagnosis of axillary lymph node metastases in breast cancer by spectrum analysis of radio frequency echo signals (Tateishi), 1151

Brevetti, G., see Rengo, C.
Brinkman, H. J. F., see Ursem, N. T. C.
Brook, F., see Chan, S.-T.
Brook, F., see Ying, M.
Brown, B., see Chan, S.-T.
Brown, J. M., Quedens-Case, C., Alderman, J. L., Greener, Y. and Taylor, K. J. W.: contrast-enhanced sonography of tumor neovascularity in a rabbit model, 495
Brown, J. M., see Holland, C. K.
Brown, N. A., see Ramnarine, K. V.
Brown, S. L., see Fowlkes, J. B.
Bruining, N., Von Birgelen, C., De Feyter, P. J., Ligthart, J., Serruys, P. W. and Roelandt, J. R. T. C.: dynamic imaging of coronary stent structures:

an ECG-gated three-dimensional intracoronary ultrasound study in humans, 631
Bruschke, A. V. G., see de Groot, E.

Bubble stability
experimental study of stability of a contrast agent in an ultrasound field (Wu), 257

Bubbles
dynamic behavior of bubbles during extracorporeal shock-wave lithotripsy (Kodama), 1227 (Erratum),
dynamic behavior of bubbles during extracorporeal shock-wave lithotripsy (Kodama), 723
experimental study of stability of a contrast agent in an ultrasound field (Wu), 257
extracorporeal shock waves act by shock wave-gas bubble interaction (Delius), 1055
innovative technology for tissue disruption by explosive-induced shock waves (Kodama), 1459

C

Céspedes, E. I., see de Korte, C. L.
Céspedes, I., see Li, W.
Cachard, C., see Bouzakaz, A.
Cachard, C., see Finet, G.
Cala, S. J., Kenyon, C. M., Lee, A., Watkin, K., Macklem, P. T. and Rochester, D. F.: respiratory ultrasonography of human parasternal intercostal muscle *in vivo*, 313

Calibration
3-D sonographic volume measurement of the cerebral ventricular system: *in vitro* validation (Kampmann), 1169
a new method for measuring the effective radiating area of physiotherapy treatment heads (Zeqiri), 761
a simple and accurate formula for the sound velocity in water (Lubbers), 1065
analysis of linear, area and volume distortion in 3D ultrasound imaging (Tong), 355
in vitro evaluation of three-dimensional ultrasonography based on magnetic scanhead tracking (Gilja), 1161
rapid calibration for 3-D freehand ultrasound (Prager), 855
the NPL Doppler fetal heart beat detector test facility (Bond), 443
validation of a new blood-mimicking fluid for use in Doppler flow test objects (Ramnarine), 451

Cancer
3-D colour Doppler image quantification of breast masses (Carson), 945
analysis of blood flow in adnexal tumors by using color Doppler imaging and pulsed spectral analysis (Takac), 1137
atlas of ultrasound and ductal echography of the breast (Fonda), 925
contrast-enhanced sonography of tumor neovascularity in a rabbit model (Brown), 495

in vitro diagnosis of axillary lymph node metastases in breast cancer by spectrum analysis of radio frequency echo signals (Tateishi), 1151
ultrasonographic evaluation of small cervical lymph nodes in head and neck cancer (Yoshida), 621

Caps, M., see Jong, J.-M.
Caps, M., see Vaezy, S.

Cardiac function
portal vein pulsatility ratio provides a measure of right heart function in chronic heart failure (Rengo), 327

Cardinal, H. N., see Tong, S.

Cardioembolic stroke
oscillating thromboemboli within the extracranial internal carotid artery demonstrated by ultrasonography in patients with acute cardioembolic stroke (Kimura), 1121

Cardoso, R., see Bernardino, F.

Carotid artery
assessment of carotid wall motion and stiffness with tissue Doppler imaging (Schmidt-Trucksäss), 639
automated intima-media thickness: The Los Angeles Atherosclerosis Study (Dwyer), 981
blood-flow velocities and their relationships in carotid and middle cerebral arteries (Nagai), 1131
influence of ECG-triggered data acquisition on reliability for carotid plaque volume measurements with a magnetic sensor three-dimensional ultrasound system (Delcker), 601
oscillating thromboemboli within the extracranial internal carotid artery demonstrated by ultrasonography in patients with acute cardioembolic stroke (Kimura), 1121
the development of hemodynamics in the extracranial carotid and vertebral arteries (Schöning), 655
ultrasonographic characterization of carotid plaques (Montauban van Swijndregt), 489
ultrasound imaging for arterial wall thickness measurement: an *in vitro* study with stereomicroscopic correlation (Raninen), 833

Carson, P. L., Fowlkes, J. B., Roubidoux, M. A., Moskalik, A. P., Govil, A., Normolle, D., LeCarpentier, G., Nattakom, S., Helvie, M. and Rubin, J. M.: 3-D colour Doppler image quantification of breast masses, 945
Carter, S., see Vaezy, S.

Cartilage
automatic three-dimensional reconstruction and characterization of articular cartilage from high-resolution ultrasound acquisitions (Lefebvre), 1369
evaluation of acoustical parameter sensitivity to age-related and osteoarthritic changes in articular cartilage using 50-MHZ ultrasound (Chérin), 341

Cathignol, D., see Arefiev, A.
Cathignol, D., see Lafon, C.

Cavitation
artificial cavitation nuclei significantly enhance acoustically induced cell transfection (Greenleaf), 587

effect of acoustic cavitation on platelets in the presence of an echo-contrast agent (Everbach), 129
defects generated in human stratum corneum specimens by ultrasound (Wu), 705
demonstration of potential noninvasive ultrasound brain therapy through an intact skull (Hynynen), 275
enhancement of ultrasonically-induced hemolysis by perfluorocarbon-based compared to air-based echo-contrast agents (Miller), 285
gas-body-based contrast agent enhances vascular bioeffects of 1.09 MHz ultrasound on mouse intestine (Miller), 1201
the interaction of ultrasonic heating and cavitation in vascular bioeffects on mouse intestine (Miller), 123

Cell function
ultrasound inhibits the adhesion and migration of smooth muscle cells *in vitro* (Alter), 711

Cells
an investigation of possible effects of high-frequency ultrasound on cellular integrity of cultured fibroblasts (Chandraratna), 911
enhancement of ultrasonically-induced hemolysis by perfluorocarbon-based compared to air-based echo-contrast agents (Miller), 285
evaluation of acoustic properties of the live human smooth-muscle cell using scanning acoustic microscopy (Kinoshita), 1397
sonochemicals increase the mutation frequency of V79 cells *in vitro* (Doida), 1209
ultrasound inhibits the adhesion and migration of smooth muscle cells *in vitro* (Alter), 711

Cellular integrity
an investigation of possible effects of high-frequency ultrasound on cellular integrity of cultured fibroblasts (Chandraratna), 911

Cerebral blood flow
a new 1-MHz probe for transcranial Doppler sonography in patients with inadequate temporal bone windows (Klötzsch), 101

Cervical lymph node
ultrasonographic evaluation of small cervical lymph nodes in head and neck cancer (Yoshida), 621

Chérin, E., Saïed, A., Laugier, P., Netter, P. and Berger, G.: evaluation of acoustical parameter sensitivity to age-related and osteoarthritic changes in articular cartilage using 50-MHZ ultrasound, 341
Chan, C. H., see Jong, J.-M.
Chan, S.-T., Brook, F., Ahuja, A., Brown, B. and Metreweli, C.: alteration of thyroid blood flow during the normal menstrual cycle in healthy Chinese women, 15
Chandraratna, N., see Anthony, P.
Chapelon, J. Y., see Arefiev, A.
Chapelon, J. Y., see Lafon, C.
Chappelow, J., see Wu, J.

Characterisation
an *in vivo* method for measuring the mechanical properties of the skin using ultrasound (Diridollou), 215

in vitro investigation of lymph node metastasis of colorectal cancer using ultrasonic spectral parameters (Noritomi), 235
quantification of sonographic echogenicity with grey-level histogram width: a clinical tissue characterization (Maeda), 225

Chen, C.-Y., see Hsu, W.-H.
Chen, L., ter Haar, G., Hill, C. R., Eccles, S. A. and Box, G.: treatment of implanted liver tumors with focused ultrasound, 1475
Chen, M.-F., see Lin, L.-C.
Chen, W.-J., see Lin, L.-C.
Chérin, E., see Lefebvre, F.
Chi, E. Y., see Vaezy, S.
Chiang, C.-D., see Hsu, W.-H.

Chinese
alteration of thyroid blood flow during the normal menstrual cycle in healthy Chinese women (Chan), 15

Christopher, D. A., see Aristizábal, O.

Circle of Willis
a new 1-MHz probe for transcranial Doppler sonography in patients with inadequate temporal bone windows (Klötzsch), 101

Clarke, R. L., see Meaney, P. M.
Cleveland, R. O., Lifshitz, D. A., Connors, B. A., Evan, A. P., Willis, L. R. and Crum, L. A.: *in vivo* pressure measurements of lithotripsy shock waves in pigs, 293
Cloutier, G., see Qin, Z.
Cohen, L., see Pellerin, D.
Coleman, A. J., Draguioti, E., Tiptaf, R., Shotri, N. and Saunders, J. E.: acoustic performance and clinical use of a fibreoptic hydrophone, unusual pseudoaneurysms after catheterization: successful treatment by ultrasound-guided compression (Do), 377
Coleman, D. J., see Deng, C. X.

Color Doppler energy
factors affecting color Doppler energy ultrasound recordings in an *in-vitro* model (Gudmundsson), 899

Color Doppler
analysis of blood flow in adnexal tumors by using color Doppler imaging and pulsed spectral analysis (Takac), 1137
blood flow through the ductus venosus in human fetus: calculation using Doppler velocimetry and computational findings (Pennati), 477
color Doppler sonography of normal breasts: detectability of arterial blood vessels and typical flow patterns (Rettenbacher), 1307
color Doppler ultrasound pulsatile flow signals of thoracic lesions: comparison of lung cancers and benign lesions (Hsu), 1087
the development of hemodynamics in the extracranial carotid and vertebral arteries (Schöning), 655

Color flow mapping
an acoustic injection test object for colour flow imaging systems (Li), 161
color flow mapping (Alam), 607
in response to K. Ferrara (Alam), 612

in response to S. K. Alam and K. J. Parker (Ferrara), 611

Color imaging
diagnosis and monitoring of middle cerebral artery occlusion with contrast-enhanced transcranial color-coded real-time sonography in patients with inadequate acoustic bone windows (Postert), 333

Connors, B. A., see Cleveland, R. O.

Contour analysis
evaluation of model-based processing algorithms for averaged transmitral spectral Doppler images (Hall), 55
reliability and reproducibility of automated contour analysis in intravascular ultrasound images of femoropopliteal arteries (van der Lugt), 43

Constitution
World Federation for Ultrasound in Medicine and Biology Constitution, 931

Contractility
color Doppler imaging of the myocardium: current status and potential clinical applications (Ofili), 177

Contrast media
acoustic modeling of shell-encapsulated gas bubbles (Frinking), 523
advances in echo imaging using contrast enhancement (Senior), 1511
advantages of subharmonic over second harmonic backscatter for contrast-to-tissue echo enhancement (Shankar), 395
artificial cavitation nuclei significantly enhance acoustically induced cell transfection (Greenleaf), 587
effect of acoustic cavitation on platelets in the presence of an echo-contrast agent (Everbach), 129
contrast-enhanced sonography of tumor neovascularity in a rabbit model (Brown), 495
conventional and hypobaric activation of an ultrasound contrast agent (Forsberg), 1143
diagnosis and monitoring of middle cerebral artery occlusion with contrast-enhanced transcranial color-coded real-time sonography in patients with inadequate acoustic bone windows (Postert), 333
dissolution of multicomponent microbubbles in the bloodstream: 1. Theory (Kabalnov), 739
dissolution of multicomponent microbubbles in the bloodstream: 2. Experiment (Kabalnov), 751
echo contrast-enhanced three-dimensional power Doppler of intracranial arteries (Postert), 953
enhancement of ultrasonically-induced hemolysis by perfluorocarbon-based compared to air-based echo-contrast agents (Miller), 285
experimental study of stability of a contrast agent in an ultrasound field (Wu), 257
gas-body-based contrast agent enhances vascular bioeffects of 1.09 MHz ultrasound on mouse intestine (Miller), 1201
imaging and spectrum analysis of contrast agents in the *in vivo* rabbit eye using very-high-frequency ultrasound (Deng), 383
improved investigation of portal-hepatic veins by echo-enhanced Doppler sonography (Fischer), 1345

improved quantification of myocardial mass by three-dimensional echocardiography using a deposit contrast agent (Kasprzak), 647
measurements of the nonlinearity parameter B/A of contrast agents (Wu), 153
onset delay of acoustic second harmonic backscatter from bubbles or microspheres (Zheng), 513
quantification of the enhanced backscatter phenomenon from an intravenous and an intra-arterial contrast agent (Moran), 871
sonochemicals increase the mutation frequency of V79 cells *in vitro* (Doida), 1209
standard properties of ultrasound contrast agents (Bouzakaz), 469
temperature rise generated by ultrasound in the presence of contrast agent (Wu), 267
ultrasound contrast agents (Perkins), 307

Contrast
advantages of subharmonic over second harmonic backscatter for contrast-to-tissue echo enhancement (Shankar), 395
an analysis of elastographic contrast-to-noise ratio (Varghese), 915
limits on the contrast of strain concentrations in elastography (Kallel), 1215

Coronary artery
artifacts in intravascular ultrasound imaging during coronary artery stent implantation (Finet), 793
automated intima-media thickness: The Los Angeles Atherosclerosis Study (Dwyer), 981
dynamic imaging of coronary stent structures: an ECG-gated three-dimensional intracoronary ultrasound study in humans (Bruining), 631
ultrasonic tissue characterization for coronary care unit patients with acute myocardial infarction (Lin), 187

Cox, C., see Doida, Y.
Cromeens, D. M., see Stafford, R. J.
Crum, L. A., see Cleveland, R. O.
Crum, L., see Vaezy, S.

D

D'Amato, T., see Rengo, C.
Dams, J., see Suhm, N.
De Feyter, P. J., see Bruining, N.
de Groot, E., Zwinderman, A. H., van der Steen, A. F. W., Ackerstaff, R. G. A., Montauban van Swijndregt, A. D., Bom, N., Lie, K. I. and Bruschke, A. V. G.: variance components analysis of carotid and femoral intima-media thickness measurements, 825
de Jong, N., see Bouzakaz, A.
de Jong, N., see Frinking, P. J. A.
de Korte, C. L., van der Steen, A. F. W., Céspedes, E. I. and Pasterkamp, G.: intravascular ultrasound elastography in human arteries: initial experience *in vitro*, 401
de Lange, E. E., see Bakker, J.
de Letter, J., see Montauban van Swijndregt, A. D.
Delachartre, Ph., see Finet, G.
Delahunt, T. A., see Geelkerken, R. H.
Delcker, A. and Tegeler, C.: influence of ECG-triggered data acquisition on

reliability for carotid plaque volume measurements with a magnetic sensor three-dimensional ultrasound system, 601
Delius, M., Ueberle, F. and Eisenmenger, W.: extracorporeal shock waves act by shock wave-gas bubble interaction, 1055
Deng, C. X., Lizzi, F. L., Silverman, R. H., Ursea, R. and Coleman, D. J.: imaging and spectrum analysis of contrast agents in the *in vivo* rabbit eye using very-high-frequency ultrasound, 383

Diastolic function
beat averaging alternatives for transmitral Doppler flow velocity images (Hall), 971
color Doppler imaging of the myocardium: current status and potential clinical applications (Ofili), 177
evaluation of model-based processing algorithms for averaged transmitral spectral Doppler images (Hall), 55

Dichorionicity
fetal biometry and outcome in monochorionic vs. dichorionic twin pregnancies; a retrospective cross-sectional matched-control study (Snijder), 197
Diridollou, S., Berson, M., Vabre, V, Black, D., Karlsson, B., Auriol, F., Gregoire, J. M., Yvon, C., Vaillant, L., Gall, Y. and Patat, F.: an *in vivo* method for measuring the mechanical properties of the skin using ultrasound, 215

Dissolution kinetics
dissolution of multicomponent microbubbles in the bloodstream: 1. Theory (Kabalnov), 739
dissolution of multicomponent microbubbles in the bloodstream: 2. Experiment (Kabalnov), 751

Distensibility
a noninvasive method to estimate pulse wave velocity in arteries locally by means of ultrasound (Brands), 1325
bladder filling reduces femoral artery wall distension and strain: beware of a full bladder! (Willekes), 803
effect of timing of blood pressure measurement in the assessment of arterial stiffness: The SMART Study (Simons), 1285

Distension
bladder filling reduces femoral artery wall distension and strain: beware of a full bladder! (Willekes), 803

Distortion
analysis of linear, area and volume distortion in 3D ultrasound imaging (Tong), 355
Do, Y., see Anthony, P.
Dobonici, G., see Kröger, K.
Doida, Y., Marcello, K. R., Brayman, A. A., Cox, C., Barned, S. and Miller, M. W.: sonochemicals increase the mutation frequency of V79 cells *in vitro*, 1209
Dong, F., see Madsen, E. L.

Doppler power
in situ measurements of Doppler power vs. flow turbulence intensity in red cell suspensions (Wu), 1009

Doppler signal processing
a brief history of Doppler ultrasound in the diagnosis of peripheral vascular disease (Sigel), 169
in vivo validation of the time domain velocity measurement technique of blood flow in human fetuses (Alcázar), 9
umbilical artery waveform analysis based on maximum, mean and mode velocity in early human pregnancy (Ursem), 1

Doppler tissue imaging
pre-ejectional left ventricular wall motions studied on conscious dogs using Doppler myocardial imaging: relationships with indices of left ventricular function (Pellerin), 1271

Doppler
3-D colour Doppler image quantification of breast masses (Carson), 945
40-MHz echocardiography scanner for cardiovascular assessment of mouse embryos (Aristizábal), 1407
a brief history of Doppler ultrasound in the diagnosis of peripheral vascular disease (Sigel), 169
a new 1-MHz probe for transcranial Doppler sonography in patients with inadequate temporal bone windows (Klötzsch), 101
a noninvasive method to estimate pulse wave velocity in arteries locally by means of ultrasound (Brands), 1325
aliasing-tolerant color Doppler quantification of regurgitant jets (Stewart), 881
alteration of thyroid blood flow during the normal menstrual cycle in healthy Chinese women (Chan), 15
an acoustic injection test object for colour flow imaging systems (Li), 161
analysis of blood flow in adnexal tumors by using color Doppler imaging and pulsed spectral analysis (Takac), 1137
assessment of carotid wall motion and stiffness with tissue Doppler imaging (Schmidt-Trucksäss), 639
atlas of ultrasound and ductal echography of the breast (Fonda), 925
beat averaging alternatives for transmitral Doppler flow velocity images (Hall), 971
blood flow through the ductus venosus in human fetus: calculation using Doppler velocimetry and computational findings (Pennati), 477
blood velocity profile in the ductus venosus inlet expressed by the mean/maximum velocity ratio (Kiserud), 1301
color Doppler imaging of the myocardium: current status and potential clinical applications (Ofili), 177
color Doppler ultrasound pulsatile flow signals of thoracic lesions: comparison of lung cancers and benign lesions (Hsu), 1087
duodenal meal stimulation leads to coeliac artery vasoconstriction and superior mesenteric artery vasodilatation: an intra-abdominal ultrasound study (Geelkerken), 1351
estimation of the human liver volume and configuration using three-dimensional ultrasonography: effect of a high-caloric liquid meal (Hausken), 1357
evaluation of model-based processing algorithms for averaged transmitral spectral Doppler images (Hall), 55
factors affecting color Doppler energy ultrasound recordings in an in-vitro model (Gudmundsson), 899
Gosling's Doppler pulsatility index revisited (Michel), 597

improved investigation of portal-hepatic veins by echo-enhanced Doppler sonography (Fischer), 1345
in situ measurements of Doppler power vs. flow turbulence intensity in red cell suspensions (Wu), 1009
in vivo validation of the time domain velocity measurement technique of blood flow in human fetuses (Alcázar), 9
kinetics of the "Black Hole" phenomenon in ultrasound backscattering measurements with red blood cell aggregation (Qin), 245
lower extremity volumetric arterial blood flow in normal subjects (Holland), 1079
multilevel and motion model-based ultrasonic speckle tracking algorithms (Yeung), 427
portal vein pulsatility ratio provides a measure of right heart function in chronic heart failure (Rengo), 327
post-graduate course in vascular Doppler: a comprehensive course on videotapes (Duck), 613
pre-ejectional left ventricular wall motions studied on conscious dogs using Doppler myocardial imaging: relationships with indices of left ventricular function (Pellerin), 1271
quantification of iliac artery stenoses: a methodological comparative study between intravascular ultrasound, arteriography and duplex scanning (Vogt), 963
the narrow band hypothesis: an interesting approach for high-intensity transient signals (HITS) detection (Roy), 375
the NPL Doppler fetal heart beat detector test facility (Bond), 443
time domain analysis of embolic signals can be used in place of high-resolution Wigner analysis when classifying gaseous and particulate emboli (Smith), 989
umbilical artery waveform analysis based on maximum, mean and mode velocity in early human pregnancy (Ursem), 1
validation of a new blood-mimicking fluid for use in Doppler flow test objects (Ramnarine), 451
vibration sonoelastography and the detectability of lesions (Parker), 1437

Downey, D. B., see Tong, S.
Downing, L. J., see Fowlkes, J. B.
Draguioti, E., see Coleman, A. J.
Dubiel, M., see Gudmundsson, S.
Duck, F. A.: post-graduate course in vascular Doppler: a comprehensive course on videotapes, 613

Ductal imaging
atlas of ultrasound and ductal echography of the breast (Fonda), 925

Ductus venosus
blood flow through the ductus venosus in human fetus: calculation using Doppler velocimetry and computational findings (Pennati), 477
blood velocity profile in the ductus venosus inlet expressed by the mean/maximum velocity ratio (Kiserud), 1301

Duggan, P.: introduction to ultrasound, 926
Durand, L.-G., see Qin, Z.
Dwyer, J. H., Sun, P., Kwong-Fu, H., Dwyer, K. M. and Selzer, R. H.: automated intima-media thickness: The Los Angeles Atherosclerosis Study, 981

Dwyer, K. M., see Dwyer, J. H.
Dwyer-Joyce, L., see Lee, D. J.

E

Earley, C. J., see Nagai, Y.
Eccles, S. A., see Chen, L.

ECG gated
dynamic imaging of coronary stent structures: an ECG-gated three-dimensional intracoronary ultrasound study in humans (Bruining), 631
influence of ECG-triggered data acquisition on reliability for carotid plaque volume measurements with a magnetic sensor three-dimensional ultrasound system (Delcker), 601

Echocardiography
40-MHz echocardiography scanner for cardiovascular assessment of mouse embryos (Aristizábal), 1407
aliasing-tolerant color Doppler quantification of regurgitant jets (Stewart), 881
beat averaging alternatives for transmitral Doppler flow velocity images (Hall), 971
color Doppler imaging of the myocardium: current status and potential clinical applications (Ofili), 177
dissolution of multicomponent microbubbles in the bloodstream: 1. Theory (Kabalnov), 739
dissolution of multicomponent microbubbles in the bloodstream: 2. Experiment (Kabalnov), 751
enhancement of ultrasonically-induced hemolysis by perfluorocarbon-based compared to air-based echo-contrast agents (Miller), 285
evaluation of model-based processing algorithms for averaged transmitral spectral Doppler images (Hall), 55
pre-ejectional left ventricular wall motions studied on conscious dogs using Doppler myocardial imaging: relationships with indices of left ventricular function (Pellerin), 1271
quantification of the enhanced backscatter phenomenon from an intravenous and an intra-arterial contrast agent (Moran), 871

Echogenicity
the value of thyroid parenchymal echogenicity as an indicator of pathology using the sternomastoid muscle for comparison (Ying), 1097
ultrasound echogenicity in experimental venous thrombosis (Fowlkes), 1175

Edwards, M. J., see Horder, M. M.
Eisenmenger, W., see Delius, M.

Elastic modulus
a new elastographic method for estimation and imaging of lateral displacements, lateral strains, corrected axial strains and Poisson's ratios in tissues (Konofagou), 1183

Elasticity
a new elastographic method for estimation and imaging of lateral displacements, lateral strains, corrected axial strains and Poisson's ratios in tissues (Konofagou), 1183

an *in vivo* method for measuring the mechanical properties of the skin using ultrasound (Diridollou), 215
elastographic imaging of low-contrast elastic modulus distributions in tissue (Kallel), 409
intravascular ultrasound elastography in human arteries: initial experience *in vitro* (de Korte), 401
multilevel and motion model-based ultrasonic speckle tracking algorithms (Yeung), 427
shear wave elasticity imaging: a new ultrasonic technology of medical diagnostics (Sarvazyan), 1419
vibration sonoelastography and the detectability of lesions (Parker), 1437
ultrasonic and viscoelastic properties of skin under transverse mechanical stress *in vitro* (Pan), 995

Elastography
a new elastographic method for estimation and imaging of lateral displacements, lateral strains, corrected axial strains and Poisson's ratios in tissues (Konofagou), 1183
an analysis of elastographic contrast-to-noise ratio (Varghese), 915
characterization of elastographic noise using the envelope of echo signals (Varghese), 543
elastographic imaging of low-contrast elastic modulus distributions in tissue (Kallel), 409
elastographic imaging of thermal lesions in soft tissue: a preliminary study *in vitro* (Stafford), 1449
intravascular ultrasound elastography in human arteries: initial experience *in vitro* (de Korte), 401
limits on the contrast of strain concentrations in elastography (Kallel), 1215
shear wave elasticity imaging: a new ultrasonic technology of medical diagnostics (Sarvazyan), 1419
vibration sonoelastography and the detectability of lesions (Parker), 1437

Elbers, H. R. J., see Montauban van Swijndregt, A. D.
Elliott, P. D., see Kawchuk, G. N.

Embolism
the narrow band hypothesis: an interesting approach for high-intensity transient signals (HITS) detection (Roy), 375
time domain analysis of embolic signals can be used in place of high-resolution Wigner analysis when classifying gaseous and particulate emboli (Smith), 989

Embryo
40-MHz echocardiography scanner for cardiovascular assessment of mouse embryos (Aristizábal), 1407
effects of pulsed ultrasound on embryonic development: an *in vitro* study (Ramnarine), 575

Emelianov, S. Y., see Sarvazyan, A. P.

Endoscopy
design and preliminary results of an ultrasound applicator for interstitial thermal coagulation (Lafon), 113

Epstein-Plesset
dissolution of multicomponent microbubbles in the bloodstream: 1. Theory (Kabalnov), 739

dissolution of multicomponent microbubbles in the bloodstream: 2. Experiment (Kabalnov), 751

Errors
3-D sonographic volume measurement of the cerebral ventricular system: *in vitro* validation (Kampmann), 1169
acoustic modeling of shell-encapsulated gas bubbles (Frinking), 523
analysis of linear, area and volume distortion in 3D ultrasound imaging (Tong), 355
artifacts in intravascular ultrasound imaging during coronary artery stent implantation (Finet), 793
automated intima-media thickness: The Los Angeles Atherosclerosis Study (Dwyer), 981
in vitro evaluation of three-dimensional ultrasonography based on magnetic scanhead tracking (Gilja), 1161
in vitro measurement of kidney size: comparison of ultrasonography and MRI (Bakker), 683
influence of ECG-triggered data acquisition on reliability for carotid plaque volume measurements with a magnetic sensor three-dimensional ultrasound system (Delcker), 601
intra- and inter-observer variability and reliability of prostate volume measurement via two-dimensional and three-dimensional ultrasound imaging (Tong), 673
intraobserver and interobserver variance in the measurement of ultrasound-estimated bladder weight (Naya), 771
SieScape™: a new sonographic dimension with fictive images (Kröger), 1125
the NPL Doppler fetal heart beat detector test facility (Bond), 443
ultrasound imaging for arterial wall thickness measurement: an *in vitro* study with stereomicroscopic correlation (Raninen), 833
validation of a new blood-mimicking fluid for use in Doppler flow test objects (Ramnarine), 451
variance components analysis of carotid and femoral intima-media thickness measurements (de Groot), 825

Erythrocytes
kinetics of the "Black Hole" phenomenon in ultrasound backscattering measurements with red blood cell aggregation (Qin), 245

ESWL
extracorporeal shock waves act by shock wave-gas bubble interaction (Delius), 1055
in vivo pressure measurements of lithotripsy shock waves in pigs (Cleveland), 293
innovative technology for tissue disruption by explosive-induced shock waves (Kodama), 1459

Evan, A. P., see Cleveland, R. O.
Evans, D. H., see Smith, J. L.
Everbach, E. C., Makin, I. R. S., Francis, C. W. and Meltzer, R. S.: effect of acoustic cavitation on platelets in the presence of an echo-contrast agent, 129

Explosive
innovative technology for tissue disruption by explosive-induced shock waves (Kodama), 1459

Exposimetry
a 3-D finite-element model for computation of temperature profiles and regions of thermal damage during focused ultrasound surgery exposures (Meaney), 1489
acoustic performance and clinical use of a fibreoptic hydrophone (Coleman), 143
enhancement of ultrasonically-induced hemolysis by perfluorocarbon-based compared to air-based echo-contrast agents (Miller), 285
in vivo pressure measurements of lithotripsy shock waves in pigs (Cleveland), 293
magnetic resonance imaging of ultrasonic fields (Walker), 137

Extended field of view
SieScape™: a new sonographic dimension with fictive images (Kröger), 1125
vein graft surveillance with scanhead tracking duplex ultrasound imaging: a preliminary report (Jong), 1313

Eye
imaging and spectrum analysis of contrast agents in the *in vivo* rabbit eye using very-high-frequency ultrasound (Deng), 383

F

Federlein, J., see Postert, T.

Feeding
duodenal meal stimulation leads to coeliac artery vasoconstriction and superior mesenteric artery vasodilatation: an intra-abdominal ultrasound study (Geelkerken), 1351
estimation of the human liver volume and configuration using three-dimensional ultrasonography: effect of a high-caloric liquid meal (Hausken), 1357

Feleppa, E. J., see Lee, D. J.
Feleppa, E. J., see Noritomi, T.
Feleppa, E. J., see Tateishi, T.

Femoral
reliability and reproducibility of automated contour analysis in intravascular ultrasound images of femoropopliteal arteries (van der Lugt), 43
ultrasound imaging for arterial wall thickness measurement: an *in vitro* study with stereomicroscopic correlation (Raninen), 833

Femoropopliteal arteries
reliability and reproducibility of automated contour analysis in intravascular ultrasound images of femoropopliteal arteries (van der Lugt), 43

Fenster, A., see Tong, S.
Ferrara, K. W., see Zagar, B. G.
Ferrara, K.: in response to S. K. Alam and K. J. Parker, 611 (Letter)
Ferrazzi, E., see Pennati, G.

Fetal aorta
in vivo validation of the time domain velocity measurement technique of blood flow in human fetuses (Alcázar), 9

Fetal biometry
fetal biometry and outcome in monochorionic vs. dichorionic twin pregnancies; a retrospective cross-sectional matched-control study (Snijder), 197

Fetal birth weight
fetal biometry and outcome in monochorionic vs. dichorionic twin pregnancies; a retrospective cross-sectional matched-control study (Snijder), 197

Fetal flow
in vivo validation of the time domain velocity measurement technique of blood flow in human fetuses (Alcázar), 9
umbilical artery waveform analysis based on maximum, mean and mode velocity in early human pregnancy (Ursem), 1

Fetal heart detector
the NPL Doppler fetal heart beat detector test facility (Bond), 443

Fetal nuchal translucency
semiautomated ultrasonographic measurement of fetal nuchal translucency using a computer software tool (Bernardino), 51

Feto-fetal transfusion
fetal biometry and outcome in monochorionic vs. dichorionic twin pregnancies; a retrospective cross-sectional matched-control study (Snijder), 197

Fetus
blood flow through the ductus venosus in human fetus: calculation using Doppler velocimetry and computational findings (Pennati), 477
blood velocity profile in the ductus venosus inlet expressed by the mean/maximum velocity ratio (Kiserud), 1301
fetal biometry and outcome in monochorionic vs. dichorionic twin pregnancies; a retrospective cross-sectional matched-control study (Snijder), 197
in vivo heating of the guinea-pig fetal brain by pulsed ultrasound and estimates of thermal index (Horder), 1467
ultrasound-induced temperature increase in guinea-pig fetal brain *in utero*: third-trimester gestation (Horder), 1501
ultrasound-induced temperature increase in the guinea-pig fetal brain *in vitro* (Horder), 697

Fibreoptic hydrophone
acoustic performance and clinical use of a fibreoptic hydrophone (Coleman), 143

Fibroblasts
an investigation of possible effects of high-frequency ultrasound on cellular integrity of cultured fibroblasts (Chandraratna), 911

Fictive images
SieScape™: a new sonographic dimension with fictive images (Kröger), 1125

Finet, G., Cachard, C., Delachartre, Ph., Maurincomme, E. and Beaune, J.: artifacts in intravascular ultrasound imaging during coronary artery stent implantation, 793
Fischer, G., Rak, R. and Sackmann, M.: improved investigation of portal-hepatic veins by echo-enhanced Doppler sonography, 1345

Flaim, S., see Kabalnov, A.

Flexors
multilevel and motion model-based ultrasonic speckle tracking algorithms (Yeung), 427

Flow
blood flow imaging and volume flow quantitation with intravascular ultrasound (Li), 203
blood-flow velocities and their relationships in carotid and middle cerebral arteries (Nagai), 1131
color Doppler ultrasound pulsatile flow signals of thoracic lesions: comparison of lung cancers and benign lesions (Hsu), 1087
contrast-enhanced sonography of tumor neovascularity in a rabbit model (Brown), 495
in situ measurements of Doppler power vs. flow turbulence intensity in red cell suspensions (Wu), 1009
lower extremity volumetric arterial blood flow in normal subjects (Holland), 1079
portal vein pulsatility ratio provides a measure of right heart function in chronic heart failure (Rengo), 327

Fonda, J.: atlas of ultrasound and ductal echography of the breast, 925

Force vectors
respiratory ultrasonography of human parasternal intercostal muscle *in vivo* (Cala), 313

Fornaris, R. J., see Zagar, B. G.
Forsberg, F., Roy, R., Merton, D. A., Rawool, N. M., Liu, J.-B., Huang, M., Kessler, D. and Goldberg, B. B.: conventional and hypobaric activation of an ultrasound contrast agent, 1143
Forsberg, F., see Molthen, R. C.
Foster, F. S., see Aristizábal, O.
Foster, F. S., see Pan, L.
Foster, F. S., see Walker, C. L.
Fowlkes, J. B., see Carson, P. L.
Fowlkes, J. B., see Sarvazyan, A. P.
Fowlkes, J. B., Strieter, R. M., Downing, L. J., Brown, S. L., Saluja, A., Salles-Cunha, S., Kadell, A. M., Wrobleski, S. K. and Wakefield, T. W.: ultrasound echogenicity in experimental venous thrombosis, 1175
Francis, C. W., see Everbach, E.
Frank, G. R., see Madsen, E. L.
Frinking, P. J. A. and de Jong, N.: acoustic modeling of shell-encapsulated gas bubbles, 523
Fu, D., see Parker, K. J.
Fumero, R., see Pennati, G.

G

Gahtan, V., see Lee, D. J.
Gall, Y., see Diridollou, S.
Gallet, J., see Anthony, P.
Garra, B. S., see Wear, K. A.

Gastric motility
sonographic observations of the gastroduodenal junction in neonatal piglets (Wright), 1337

Gastroduodenal junction
sonographic observations of the gastroduodenal junction in neonatal piglets (Wright), 1337

Gee, A. H., see Prager, R. W.
Gee, A. H., see Rohling, R. N.
Geelkerken, R. H., Lamers, C. B. H. W., Delahunt, T. A., Hermans, J., Zwijsen, J. H. M. J. and van Bockel, J. H.: duodenal meal stimulation leads to coeliac artery vasoconstriction and superior mesenteric aratery vasodilatation: an intra-abdominal ultrasound study, 1351

Gene therapy
artificial cavitation nuclei significantly enhance acoustically induced cell transfection (Greenleaf), 587

Genis, V., see Molthen, R. C.
Gertner, M. R., Wilson, B. C. and Sherar, M. D.: high frequency ultrasound properties of multicellular spheroids during heating, 461
Gertner, M. R., Worthington, A. E., Wilson, B. C. and Sherar, M. D.: ultrasound imaging of thermal therapy in *in vitro* liver, 1023
Gies, R. A., see Miller, D. L.
Gilja, O. H., Hausken, T., Olafsson, S., Matre, K. and Ødegaard, S.: *in vitro* evaluation of three-dimensional ultrasonography based on magnetic scanhead tracking, 1161
Giudicelli, J.-F., see Pellerin, D.
Goldberg, B. B., see Forsberg, F.
Goldberg, B. B., see Molthen, R. C.
Goldman, B., see Hausken, T.
Goldring, M. B., see Greenleaf, W. J.
Gorry, F., see Lafon, C.

Gosling
Gosling's Doppler pulsatility index revisited (Michel), 597

Govil, A., see Carson, P. L.
Graaff, R., see Lubbers, J.
Graceswki, S. M., see Parker, K. J.
Graillat, N., see Lefebvre, F.
Grathwohl, D., see Schmidt-Trucksäss, A.
Greener, Y., see Brown, J. M.
Greenleaf, J. F., see Greenleaf, W. J.
Greenleaf, W. J., Bolander, M. E., Sarkar, G., Goldring, M. B. and Greenleaf, J. F.: artificial cavitation nuclei significantly enhance acoustically induced cell transfection, 587
Gregoire, J. M., see Diridollou, S.
Gritzmann, N., see Rettenbacher, T.
Gudmundsson, S., Valentin, L., Pirhonen, J., Olofsson, P.-A., Dubiel, M. and Marsal, K.: factors affecting color Doppler energy ultrasound recordings in an *in-vitro* model, 899

Guinea pigs
ultrasound-induced temperature increase in guinea-pig fetal brain *in utero*: third-trimester gestation (Horder), 1501

ultrasound-induced temperature increase in the guinea-pig fetal brain *in vitro* (Horder), 697

Gunawardana, R., see Anthony, P.
Gussenhoven, E. J., see van der Lugt, A.

H

ter Haar, G. R., see Meaney, P. M.
ter Haar, G., see Chen, L.
Hall, A. F., Nudelman, S. P. and Kovács, S. J.: beat averaging alternatives for transmitral Doppler flow velocity images, 971
Hall, A. F., Nudelman, S. P. and Kovacs, S. J.: evaluation of model-based processing algorithms for averaged transmitral spectral Doppler images, 55
Halpern, E. J., see Molthen, R. C.
Hanson, M. A., see Kiserud, T.

Harmonic imaging
advantages of subharmonic over second harmonic backscatter for contrast-to-tissue echo enhancement (Shankar), 395
onset delay of acoustic second harmonic backscatter from bubbles or microspheres (Zheng), 513

Hartig, B., see Schöning, M.
Hartlooper, A., see van der Lugt, A.
Hausken, T., Leotta, D. F., Helton, S., Kowdley, K. V., Goldman, B., Vaezy, S., Bolson, E. L., Sheehan, F. H. and Martin, R. W.: estimation of the human liver volume and configuration using three-dimensional ultrasonography: effect of a high-caloric liquid meal, 1357
Hausken, T., see Gilja, O. H.
Hazle, J. D., see Stafford, R. J.

Heart failure
portal vein pulsatility ratio provides a measure of right heart function in chronic heart failure (Rengo), 327

Hellvik, L. R., see Kiserud, T.
Helton, S., see Hausken, T.
Helvie, M., see Carson, P. L.

Hemolysis
enhancement of ultrasonically-induced hemolysis by perfluorocarbon-based compared to air-based echo-contrast agents (Miller), 285

Hemorrahage
the interaction of ultrasonic heating and cavitation in vascular bioeffects on mouse intestine (Miller), 123

Hemostasis
hemostasis of punctured blood vessels using high-intensity focused ultrasound (Vaezy), 903

Hepatic vein
improved investigation of portal-hepatic veins by echo-enhanced Doppler sonography (Fischer), 1345

Hepatomas
conventional and hypobaric activation of an ultrasound contrast agent (Forsberg), 1143

Hermans, J., see Geelkerken, R. H.

HIFU
a 3-D finite-element model for computation of temperature profiles and regions of thermal damage during focused ultrasound surgery exposures (Meaney), 1489
acoustic performance and clinical use of a fibreoptic hydrophone (Coleman), 143
demonstration of potential noninvasive ultrasound brain therapy through an intact skull (Hynynen), 275
dynamic behavior of bubbles during extracorporeal shock-wave lithotripsy (Kodama), 1227 (Erratum),
dynamic behavior of bubbles during extracorporeal shock-wave lithotripsy (Kodama), 723
elastographic imaging of thermal lesions in soft tissue: a preliminary study *in vitro* (Stafford), 1449
extracorporeal shock waves act by shock wave-gas bubble interaction (Delius), 1055
hemostasis of punctured blood vessels using high-intensity focused ultrasound (Vaezy), 903
in vivo pressure measurements of lithotripsy shock waves in pigs (Cleveland), 293
innovative technology for tissue disruption by explosive-induced shock waves (Kodama), 1459
treatment of implanted liver tumors with focused ultrasound (Chen), 1475
ultrasound-induced tissue ablation: studies on isolated, perfused porcine liver (Arefiev), 1033

Hill, C. R., see Chen, L.

Histogram
quantification of sonographic echogenicity with grey-level histogram width: a clinical tissue characterization (Maeda), 225

Histology
acoustic properties of atherosclerosis of human aorta obtained with high-frequency ultrasound (Saijo), 1061
elastographic imaging of thermal lesions in soft tissue: a preliminary study *in vitro* (Stafford), 1449
evaluation of acoustic properties of the live human smooth-muscle cell using scanning acoustic microscopy (Kinoshita), 1397
hemostasis of punctured blood vessels using high-intensity focused ultrasound (Vaezy), 903
high frequency ultrasound properties of multicellular spheroids during heating (Gertner), 461
in vitro diagnosis of axillary lymph node metastases in breast cancer by spectrum analysis of radio frequency echo signals (Tateishi), 1151
intravascular ultrasound elastography in human arteries: initial experience *in vitro* (de Korte), 401
quantitative ultrasonic analysis of liver metastases (Huisman), 67
treatment of implanted liver tumors with focused ultrasound (Chen), 1475

ultrasound inhibits the adhesion and migration of smooth muscle cells *in vitro* (Alter), 711
ultrasound-induced tissue ablation: studies on isolated, perfused porcine liver (Arefiev), 1033

History
a brief history of Doppler ultrasound in the diagnosis of peripheral vascular disease (Sigel), 169
history of intraoperative ultrasound (Makuuchi), 1229
interventional ultrasound in Europe (Holm), 779

HITS
the narrow band hypothesis: an interesting approach for high-intensity transient signals (HITS) detection (Roy), 375

Ho, W. L., see Hsu, W.-H.
Ho, Y.-L., see Lin, L.-C.
Hodnett, M., see Zeqiri, B.
Hoeks, A. P. G., see Brands, P. J.
Hoeks, A. P. G., see Ledoux, L. A. F.
Hoeks, A. P. G., see Willekes, C.
Holland, C. K., Brown, J. M., Scoutt, L. M. and Taylor, K. J. W.: lower extremity volumetric arterial blood flow in normal subjects, 1079
Hollerweger, A., see Rettenbacher, T.
Holm, H. H.: interventional ultrasound in Europe, 779
Honjyo, H., see Naya, Y.
Hoogland, H. J., see Willekes, C.
Hop, W. C. J., see Ursem, N. T. C.
Horder, M. M., Barnett, S. B., Vella, G. J. and Edwards, M. J.: ultrasound-induced temperatuare increase in the guinea-pig fetal brain *in vitro*, 697
Horder, M. M., Barnett, S. B., Vella, G. J., Edwards, M. J. and Wood, A. K. W.: *in vivo* heating of the guinea-pig fetal brain by pulsed ultrasound and estimates of thermal index, 1467
Horder, M. M., Barnett, S. B., Vella, G. J., Edwards, M. J. and Wood, A. K. W.: ultrasound-induced temperature increase in guinea-pig fetal brain *in utero*: third-trimester gestation, 1501
Hoskins, P. R., see Li, S. F.
Hoskins, P. R., see Ramnarine, K. V.
Hoskins, P. R.: diagnostic ultrasound - principles and instruments (5th edition)
Hsu, C.-P., see Hsu, W.-H.
Hsu, J.-Y., see Hsu, W.-H.
Hsu, W.-H., Chiang, C.-D., Chen, C.-Y., Kwan, P.-C., Hsu, J.-Y., Hsu, C.-P. and Ho, W. L.: color Doppler ultrasound pulsatile flow signals of thoracic lesions: comparison of lung cancers and benign lesions, 1087
Huang, M., see Forsberg, F.
Huisman, H. J., Thijssen, J. M., Wagener, D. J. Th. and Rosenbusch, G. J. E.: quantitative ultrasonic analysis of liver metastases, 67
Huonker, M., see Schmidt-Trucksäss, A.

Hydrophone
acoustic performance and clinical use of a fibreoptic hydrophone (Coleman), 143

Hynynen, K. and Jolesz, F. A.: demonstration of potential noninvasive ultrasound brain therapy through an intact skull, 275

Hynynen, K., see Smith, N. B.

Hyperthermia
ultrasound-induced temperature increase in guinea-pig fetal brain *in utero*: third-trimester gestation (Horder), 1501
ultrasound-induced temperature increase in the guinea-pig fetal brain *in vitro* (Horder), 697

I

Iliac
quantification of iliac artery stenoses: a methodological comparative study between intravascular ultrasound, arteriography and duplex scanning (Vogt), 963
the use of intravascular ultrasound for intraoperative assessment during semiclosed thromboendarterectomy (Vogt), 21

Image analysis
automated intima-media thickness: The Los Angeles Atherosclerosis Study (Dwyer), 981
beat averaging alternatives for transmitral Doppler flow velocity images (Hall), 971
in vitro investigation of lymph node metastasis of colorectal cancer using ultrasonic spectral parameters (Noritomi), 235
quantification of iliac artery stenoses: a methodological comparative study between intravascular ultrasound, arteriography and duplex scanning (Vogt), 963
quantification of sonographic echogenicity with grey-level histogram width: a clinical tissue characterization (Maeda), 225
the value of thyroid parenchymal echogenicity as an indicator of pathology using the sternomastoid muscle for comparison (Ying), 1097
ultrasonic tissue characterization in predicting residual ischemia and myocardial viability for patients with acute myocardial infarction (Lin), 1107
variance components analysis of carotid and femoral intima-media thickness measurements (de Groot), 825

Image processing
3-D sonographic volume measurement of the cerebral ventricular system: *in vitro* validation (Kampmann), 1169
artifacts in intravascular ultrasound imaging during coronary artery stent implantation (Finet), 793
automatic three-dimensional reconstruction and characterization of articular cartilage from high-resolution ultrasound acquisitions (Lefebvre), 1369
dynamic imaging of coronary stent structures: an ECG-gated three-dimensional intracoronary ultrasound study in humans (Bruining), 631
evaluation of model-based processing algorithms for averaged transmitral spectral Doppler images (Hall), 55
quantitative ultrasonic analysis of liver metastases (Huisman), 67
reliability and reproducibility of automated contour analysis in intravascular ultrasound images of femoropopliteal arteries (van der Lugt), 43
semiautomated segmentation of ovarian follicular ultrasound images using a knowledge-based algorithm (Sarty), 27
semiautomated ultrasonographic measurement of fetal nuchal translucency using a computer software tool (Bernardino), 51

validation of displacement measurements obtained from ultrasonic images during indentation testing (Kawchuk), 105

Imaging
3-D colour Doppler image quantification of breast masses (Carson), 945
a new elastographic method for estimation and imaging of lateral displacements, lateral strains, corrected axial strains and Poisson's ratios in tissues (Konofagou), 1183
a practical guide to ultrasound in obstetrics and gynecology (Smith), 1069
atlas of ultrasound and ductal echography of the breast (Fonda), 925
diagnostic ultrasound - a logical approach (Bradley), 925
introduction to ultrasound (Duggan), 926

Imparato, M., see Rengo, C.

in vitro *irradiation*
artificial cavitation nuclei significantly enhance acoustically induced cell transfection (Greenleaf), 587
effect of acoustic cavitation on platelets in the presence of an echo-contrast agent (Everbach), 129
design and preliminary results of an ultrasound applicator for interstitial thermal coagulation (Lafon), 113
dynamic behavior of bubbles during extracorporeal shock-wave lithotripsy (Kodama), 723
effects of pulsed ultrasound on embryonic development: an *in vitro* study (Ramnarine), 575
focused ultrasound modifications of neural circuit activity in a mammalian brain (Bachtold), 557
sonochemicals increase the mutation frequency of V79 cells *in vitro* (Doida), 1209
the feasibility of using focused ultrasound for transmyocardial revascularization (Smith), 1045
the interaction of ultrasonic heating and cavitation in vascular bioeffects on mouse intestine (Miller), 123
ultrasound imaging of thermal therapy in *in vitro* liver (Gertner), 1023
ultrasound inhibits the adhesion and migration of smooth muscle cells *in vitro* (Alter), 711
ultrasound-induced temperature increase in guinea-pig fetal brain *in utero*: third-trimester gestation (Horder), 1501
ultrasound-induced temperature increase in the guinea-pig fetal brain *in vitro* (Horder), 697

in vivo *irradiation*
application of low-intensity ultrasound to growing bone in rats (Spadaro), 567
design and preliminary results of an ultrasound applicator for interstitial thermal coagulation (Lafon), 113
design and preliminary results of an ultrasound applicator for interstitial thermal coagulation (Lafon), 113
gas-body-based contrast agent enhances vascular bioeffects of 1.09 MHz ultrasound on mouse intestine (Miller), 1201
in vivo heating of the guinea-pig fetal brain by pulsed ultrasound and estimates of thermal index (Horder), 1467
in vivo pressure measurements of lithotripsy shock waves in pigs (Cleveland), 293

the feasibility of using focused ultrasound for transmyocardial revascularization (Smith), 1045
treatment of implanted liver tumors with focused ultrasound (Chen), 1475
ultrasound-induced temperature increase in guinea-pig fetal brain *in utero*: third-trimester gestation (Horder), 1501
ultrasound-induced tissue ablation: studies on isolated, perfused porcine liver (Arefiev), 1033
in vivo *pressure measurement*
in vivo pressure measurements of lithotripsy shock waves in pigs (Cleveland), 293

Indentation
validation of displacement measurements obtained from ultrasonic images during indentation testing (Kawchuk), 105

Intercostal mechanics
respiratory ultrasonography of human parasternal intercostal muscle *in vivo* (Cala), 313

Interstitial applicator
design and preliminary results of an ultrasound applicator for interstitial thermal coagulation (Lafon), 113

Interventional ultrasound
interventional ultrasound in Europe (Holm), 779

Intima-medial thickness
automated intima-media thickness: The Los Angeles Atherosclerosis Study (Dwyer), 981
ultrasound imaging for arterial wall thickness measurement: an *in vitro* study with stereomicroscopic correlation (Raninen), 833
variance components analysis of carotid and femoral intima-media thickness measurements (de Groot), 825

Intracoronary ultrasound
dynamic imaging of coronary stent structures: an ECG-gated three-dimensional intracoronary ultrasound study in humans (Bruining), 631

Intraoperative
history of intraoperative ultrasound (Makuuchi), 1229
limitations for three-dimensional ultrasound imaging through a bore-hold trepanation (Suhm), 663
the use of intravascular ultrasound for intraoperative assessment during semiclosed thromboendarterectomy (Vogt), 21

Intraplaque hemorrhage
ultrasonographic characterization of carotid plaques (Montauban van Swijndregt), 489

Irradiation
application of low-intensity ultrasound to growing bone in rats (Spadaro), 567,
artificial cavitation nuclei significantly enhance acoustically induced cell transfection (Greenleaf), 587

design and preliminary results of an ultrasound applicator for interstitial thermal coagulation (Lafon), 113
dynamic behavior of bubbles during extracorporeal shock-wave lithotripsy (Kodama), 723
effect of acoustic cavitation on platelets in the presence of an echo-contrast agent (Everbach), 129
effects of pulsed ultrasound on embryonic development: an *in vitro* study (Ramnarine), 575
focused ultrasound modifications of neural circuit activity in a mammalian brain (Bachtold), 557
gas-body-based contrast agent enhances vascular bioeffects of 1.09 MHz ultrasound on mouse intestine (Miller), 1201
in vivo heating of the guinea-pig fetal brain by pulsed ultrasound and estimates of thermal index (Horder), 1467
in vivo pressure measurements of lithotripsy shock waves in pigs (Cleveland), 293
sonochemicals increase the mutation frequency of V79 cells *in vitro* (Doida), 1209
the feasibility of using focused ultrasound for transmyocardial revascularization (Smith), 1045
the interaction of ultrasonic heating and cavitation in vascular bioeffects on mouse intestine (Miller), 123
treatment of implanted liver tumors with focused ultrasound (Chen), 1475
ultrasound imaging of thermal therapy in *in vitro* liver (Gertner), 1023
ultrasound inhibits the adhesion and migration of smooth muscle cells *in vitro* (Alter), 711
ultrasound-induced temperature increase in guinea-pig fetal brain *in utero*: third-trimester gestation (Horder), 1501
ultrasound-induced temperature increase in the guinea-pig fetal brain *in vitro* (Horder), 697
ultrasound-induced tissue ablation: studies on isolated, perfused porcine liver (Arefiev), 1033

Ischemia
ultrasonic tissue characterization in predicting residual ischemia and myocardial viability for patients with acute myocardial infarction (Lin), 1107

IVC
ultrasound echogenicity in experimental venous thrombosis (Fowlkes), 1175

IVUS
acoustic properties of atherosclerosis of human aorta obtained with high-frequency ultrasound (Saijo), 1061
artifacts in intravascular ultrasound imaging during coronary artery stent implantation (Finet), 793
blood flow imaging and volume flow quantitation with intravascular ultrasound (Li), 203
intravascular ultrasound elastography in human arteries: initial experience *in vitro* (de Korte), 401
intravascular ultrasound imaging in coronary artery disease (van der Steen), 1511
quantification of iliac artery stenoses: a methodological comparative study between intravascular ultrasound, arteriography and duplex scanning (Vogt), 963

reliability and reproducibility of automated contour analysis in intravascular ultrasound images of femoropopliteal arteries (van der Lugt), 43
the use of intravascular ultrasound for intraoperative assessment during semiclosed thromboendarterectomy (Vogt), 21

J

Johnson, R., see Kasprzak, J. D.
Jolesz, F. A., see Hynynen, K.
Jones, J. P., see Anthony, P.
Jones, J. P., see Bachtold, M. R.
Jong, J.-M., Beach, K. W., Primozich, J. F., Bergelin, R. O., Caps, M., Chan, C. H. and Strandness, D. E. Jr.: vein graft surveillance with scanhead tracking duplex ultrasound imaging: a preliminary report, 1313
Jucha, J., see Tateishi, T.
Just, S., see Vogt, K. C.
Justin, J. R., see Lee, D. J.

K

Köster, O., see Postert, T.
Kaatee, R., see Bakker, J.
Kabalnov, A., Bradley, J., Flaim, S., Klein, D., Pelura, T., Peters, B., Otto, S., Reynolds, J., Schutt, E. and Weers, J.: dissolution of multicomponent microbubbles in the bloodstream: 2. Experiment, 751
Kabalnov, A., Klein, D., Pelura, T., Schutt, E. and Weers, J.: Dissolution of multicomponent microbubbles in the bloodstream: 1. Theory, 739
Kaczkowski, P., see Vaezy, S.
Kadell, A. M., see Fowlkes, J. B.
Kallel, F. and Ophir, J.: limits on the contrast of strain concentrations in elastography, 1215
Kallel, F., Ophir, J., Magee, K. and Krouskop, T.: elastographic imaging of low-contrast elastic modulus distributions in tissue, 409
Kallel, F., see Stafford, R. J.
Kampmann, W., Walka, M. M., Vogel, M. and Obladen, M.: 3-D sonographic volume measurement of the cerebral ventricular system: in vitro validation, 1169
Karlsson, B., see Diridollou, S.
Kasprzak, J. D., Vletter, W. B., van Meegen, J. R., Nosir, Y. F. M., Johnson, R., Ten Cate, F. J. and Roelandt, J. R. T.C.: improved quantification of myocardial mass by three-dimensional echocardiography using a deposit contrast agent, 647
Kawchuk, G. N. and Elliott, P. D.: validation of displacement measurements obtained from ultrasonic images during indentation testing, 105

K-distribution
comparison of the Rayleigh and K-distribution models using *in vivo* breast and liver tissue (Molthen), 93

Keilman, G., see Vaezy, S.
Keller, B. B., see Ursem, N. T. C.
Kemper, M. K., see Nagai, Y.
Kempski, M. H., see Ursem, N. T. C.
Kenyon, C. M., see Cala, S. J.
Kessler, D., see Forsberg, F.

Keul, J., see Schmidt-Trucksäss, A.

Kidney
elastographic imaging of low-contrast elastic modulus distributions in tissue (Kallel), 409
in vitro measurement of kidney size: comparison of ultrasonography and MRI (Bakker), 683
in vivo pressure measurements of lithotripsy shock waves in pigs (Cleveland), 293

Kihaile, P. E., see Maeda, K.
Kimura, K., Yasaka, M., Minematsu, K., Wada, K., Uchino, M., Yonemura, K., Ogata, J. and Yamaguchi, T.: oscillating thromboemboli within the extracranial internal carotid artery demonstrated by ultrasonography in patients with acute cardioembolic stroke, 1121

Kinematic models
evaluation of model-based processing algorithms for averaged transmitral spectral Doppler images (Hall), 55

Kinoshita, A., Senda, S., Mizushige, K., Masugata, H., Sakamoto, S., Kiyomoto, H. and Matsuo, H.: evaluation of acoustic properties of the live human smooth-muscle cell using scanning acoustic microscopy, 1397
Kiserud, T., Hellvik, L. R. and Hanson, M. A.: blood velocity profile in the ductus venosus inlet expressed by the man/maximum velocity ratio, 1301
Kiyomoto, H., see Kinoshita, A.
Klötzsch, C., Popescu, O. and Berlit, P.: a new 1-MHz probe for transcranial Doppler sonography in patients with inadequate temporal bone windows, 101
Klein, D., see Kabalnov, A.
Kodama, T. and Takayama K.: dynamic behavior of bubbles during extracorporeal shock-wave lithotripsy, 1227 (Erratum)
Kodama, T. and Takayama, K.: dynamic behavior of bubbles during extracorporeal shock-wave lithotripsy, 723
Kodama, T., Uenohara, H. and Takayama, K.: innovative technology for tissue disruption by explosive-induced shock waves
Kojima, M., see Naya, Y.
Konofagou, E. and Ophir, J.: a new elastographic method for estimation and imaging of lateral displacements, lateral strains, corrected axial strains and Poisson's ratios in tissues, 1183
Kovács, S. J., see Hall, A. F.
Kowdley, K. V., see Hausken, T.
Kröger, K., Massalha, K., Dobonici, G. and Rudofsky, G.: SieScape™: a new sonographic dimension with fictive images, 1125
Krishna, P. D., see Shankar, P. M.
Krouskop, T. A., see Stafford, R. J.
Krouskop, T., see Kallel, F.
Kwan, P.-C., see Hsu, W.-H.
Kwong-Fu, H., see Dwyer, J. H.

L

Lafon, C., Chapelon, J. Y., Prat, F., Gorry, F., Margonari, J., Theillére, Y. and Cathignol, D.: design and preliminary results of an ultrasound applicator for interstitial thermal coagulation, 113

Lamers, C. B. H. W., see Geelkerken, R. H.
Lancée, C. T., see Li, W.
Laparte, C., see Alcazar, J. L.
Laugier, P., see Chérin, E.
LeCarpentier, G., see Carson, P. L.
Ledoux, L. A. F., see Brands, P. J.
Ledoux, L. A. F., Willigers, J. M., Brands, P. J. and Hoeks, A. P. G.: experimental verification of the correlation behavior of analytic ultrasound radiofrequency signals received from moving structures, 1383
Lee, A., see Cala, S. J.
Lee, D. J., Sigel, B., Swami, V. K., Justin, J. R., Gahtan, V., O'Brien, S. P., Dwyer-Joyce, L., Feleppa, E. J., Roberts, A. B. and Berkowitz, H. D.: determination of carotid plaque risk by ultrasonic tissue characterization, 1291
Lee, Y.-T., see Lin, L.-C.
Lefebvre, F., Graillat, N., Chérin, E., Berger, G. and Saïed, A.: automatic three-dimensional reconstruction and characterization of articular cartilage from high-resolution ultrasound acquisitions, 1369

Left ventricle
beat averaging alternatives for transmitral Doppler flow velocity images (Hall), 971
improved quantification of myocardial mass by three-dimensional echocardiography using a deposit contrast agent (Kasprzak), 647
pre-ejectional left ventricular wall motions studied on conscious dogs using Doppler myocardial imaging: relationships with indices of left ventricular function (Pellerin), 1271
the feasibility of using focused ultrasound for transmyocardial revascularization (Smith), 1045

Left ventricular volume
improved quantification of myocardial mass by three-dimensional echocardiography using a deposit contrast agent (Kasprzak), 647

Legs
lower extremity volumetric arterial blood flow in normal subjects (Holland), 1079

Leotta, D. F., see Hausken, T.

Lesions
design and preliminary results of an ultrasound applicator for interstitial thermal coagulation (Lafon), 113
the feasibility of using focused ultrasound for transmyocardial revascularization (Smith), 1045
ultrasound-induced tissue ablation: studies on isolated, perfused porcine liver (Arefiev), 1033

Levinson, S. F., see Parker, K. J.
Levinson, S. F., see Yeung, F.
Li, S. F., Hoskins, P. R., Anderson, T. and McDicken, W. N.: an acoustic injection test object for colour flow imaging systems, 161
Li, W., see van der Lugt, A.
Li, W., van der Steen, A. F. W., Lancée, C. T., Céspedes, I. and Bom, N.: blood flow imaging and volume flow quantitation with intravascular ultrasound, 203

Liang, W., see Sarty, G. E.
Liau, C.-S., see Lin, L.-C.
Lie, K. I., see de Groot, E.
Lifshitz, D. A., see Cleveland, R. O.
Ligthart, J., see Bruining, N.

Limitations
3-D sonographic volume measurement of the cerebral ventricular system: *in vitro* validation (Kampmann), 1169
acoustic modeling of shell-encapsulated gas bubbles (Frinking), 523
analysis of linear, area and volume distortion in 3D ultrasound imaging (Tong), 355
artifacts in intravascular ultrasound imaging during coronary artery stent implantation (Finet), 793
automated intima-media thickness: The Los Angeles Atherosclerosis Study (Dwyer), 981
in vitro evaluation of three-dimensional ultrasonography based on magnetic scanhead tracking (Gilja), 1161
in vitro measurement of kidney size: comparison of ultrasonography and MRI (Bakker), 683
influence of ECG-triggered data acquisition on reliability for carotid plaque volume measurements with a magnetic sensor three-dimensional ultrasound system (Delcker), 601
intra- and inter-observer variability and reliability of prostate volume measurement via two-dimensional and three-dimensional ultrasound imaging (Tong), 673
intraobserver and interobserver variance in the measurement of ultrasound-estimated bladder weight (Naya), 771
limitations for three-dimensional ultrasound imaging through a bore-hold trepanation (Suhm), 663
SieScape™: a new sonographic dimension with fictive images (Kröger), 1125
the NPL Doppler fetal heart beat detector test facility (Bond), 443
ultrasound imaging for arterial wall thickness measurement: an *in vitro* study with stereomicroscopic correlation (Raninen), 833
validation of a new blood-mimicking fluid for use in Doppler flow test objects (Ramnarine), 451
variance components analysis of carotid and femoral intima-media thickness measurements (de Groot), 825

Lin, C.-W., see Lin, L.-C.
Lin, L.-C., Wu, C.-C., Ho, Y. L., Lin, C.-W., Chen, W.-J., Chen, M.-F., Liau, C.-S. and Lee, Y.-T.: ultrasonic tissue characterization for coronary care unit patients with acute myocardial infarction, 187
Lin, L.-C., Wu, C.-C., Ho, Y.-L., Chen, M.-F., Liau, C.-S. and Lee, Y.-T.: ultrasonic tissue characterization in predicting residual ischemia and myocardial viability for patients with acute myocardial infarction, 1107

Liquid jet
dynamic behavior of bubbles during extracorporeal shock-wave lithotripsy (Kodama), 1227 (Erratum),
dynamic behavior of bubbles during extracorporeal shock-wave lithotripsy (Kodama), 723

Lithotripsy
acoustic performance and clinical use of a fibreoptic hydrophone (Coleman), 143
dynamic behavior of bubbles during extracorporeal shock-wave lithotripsy (Kodama), 1227 (Erratum),
dynamic behavior of bubbles during extracorporeal shock-wave lithotripsy (Kodama), 723
extracorporeal shock waves act by shock wave-gas bubble interaction (Delius), 1055
in vivo pressure measurements of lithotripsy shock waves in pigs (Cleveland), 293
innovative technology for tissue disruption by explosive-induced shock waves (Kodama), 1459

Liu, J.-B., see Forsberg, F.

Liver
duodenal meal stimulation leads to coeliac artery vasoconstriction and superior mesenteric artery vasodilatation: an intra-abdominal ultrasound study (Geelkerken), 1351
improved investigation of portal-hepatic veins by echo-enhanced Doppler sonography (Fischer), 1345
estimation of the human liver volume and configuration using three-dimensional ultrasonography: effect of a high-caloric liquid meal (Hausken), 1357
quantitative ultrasonic analysis of liver metastases (Huisman), 67
treatment of implanted liver tumors with focused ultrasound (Chen), 1475
ultrasound imaging of thermal therapy in *in vitro* liver (Gertner), 1023
ultrasound-induced tissue ablation: studies on isolated, perfused porcine liver (Arefiev), 1033
using phase information in ultrasonic backscatter for *in vivo* liver analysis (Molthen), 79

Liver volume
estimation of the human liver volume and configuration using three-dimensional ultrasonography: effect of a high-caloric liquid meal (Hausken), 1357

Lizzi, F. L., see Deng, C. X.
Lorenz, A., see Suhm, N.
Lubbers, J., see Ramnarine, K. V.
Lubbers, J. and Graaff, R.: a simple and accurate formula for the sound velocity in water, 1065

Lung cancer
color Doppler ultrasound pulsatile flow signals of thoracic lesions: comparison of lung cancers and benign lesions (Hsu), 1087

Lymph node
in vitro diagnosis of axillary lymph node metastases in breast cancer by spectrum analysis of radio frequency echo signals (Tateishi), 1151
in vitro investigation of lymph node metastasis of colorectal cancer using ultrasonic spectral parameters (Noritomi), 235
ultrasonographic evaluation of small cervical lymph nodes in head and neck cancer (Yoshida), 621

M

Macheiner, P., see Rettenbacher, T.
Machi, J., see Makuuchi, M.
Machi, J., see Noritomi, T.
Machi, J., see Tateishi, T.
Macklem, P. T., see Cala, S. J.
Madsen, E. L., Frank, G. R. and Dong, F.: liquid or solid ultrasonically tissue-mimicking materials with very low scatter, 535
Maeda, K., Utsu, M. and Kihaile, P. E.: quantification of sonographic echogenicity with grey-level histogram width: a clinical tissue characterization, 225
Magee, K., see Kallel, F.
Makin, I. R. S., see Everbach, E.
Makuuchi, M., Torzilli, G. and Machi, J.: history of intraoperative ultrasound, 1229
Marcello, K. R., see Doida, Y.
Margonari, J., see Lafon, C.
Marques de Sa, J., see Bernardino, F.
Marsal, K., see Gudmundsson, S.
Martin, R. W., see Hausken, T.
Martin, R., see Vaezy, S.
Massalha, K., see Kröger, K.
Masugata, H., see Kinoshita, A.
Matre, K., see Gilja, O. H.
Matsuo, H., see Kinoshita, A.
Maurincomme, E., see Finet, G.

MCA
blood-flow velocities and their relationships in carotid and middle cerebral arteries (Nagai), 1131
diagnosis and monitoring of middle cerebral artery occlusion with contrast-enhanced transcranial color-coded real-time sonography in patients with inadequate acoustic bone windows (Postert), 333
echo contrast-enhanced three-dimensional power Doppler of intracranial arteries (Postert), 953

MCA occlusion
diagnosis and monitoring of middle cerebral artery occlusion with contrast-enhanced transcranial color-coded real-time sonography in patients with inadequate acoustic bone windows (Postert), 333

McCarthy, A., see Ramnarine, K. V.
McCarthy, L. J., see Tateishi, T.
McDicken, W. N., see Li, S. F.
McDicken, W. N., see Moran, C. M.
McKelvey, G. M., see Wright, A. B.
McLoughlin, R. F., see Tong, S.
Meaney, P. M., Clarke, R. L., ter Haar, G. R. and Rivens, I. H.: a 3-D finite-element model for computation of temperature profiles and regions of thermal damage during focused ultrasound surgery exposures, 1489

Mechanical Index
gas-body-based contrast agent enhances vascular bioeffects of 1.09 MHz ultrasound on mouse intestine (Miller), 1201

the interaction of ultrasonic heating and cavitation in vascular bioeffects on mouse intestine (Miller), 123

Mechanical properties
a new elastographic method for estimation and imaging of lateral displacements, lateral strains, corrected axial strains and Poisson's ratios in tissues (Konofagou), 1183
an *in vivo* method for measuring the mechanical properties of the skin using ultrasound (Diridollou), 215
elastographic imaging of low-contrast elastic modulus distributions in tissue (Kallel), 409
intravascular ultrasound elastography in human arteries: initial experience *in vitro* (de Korte), 401
multilevel and motion model-based ultrasonic speckle tracking algorithms (Yeung), 427
shear wave elasticity imaging: a new ultrasonic technology of medical diagnostics (Sarvazyan), 1419
ultrasonic and viscoelastic properties of skin under transverse mechanical stress *in vitro* (Pan), 995
vibration sonoelastography and the detectability of lesions (Parker), 1437

Meltzer, R. S., see Everbach E.

Menstrual cycle
alteration of thyroid blood flow during the normal menstrual cycle in healthy Chinese women (Chan), 15

Merton, D. A., see Forsberg, F.

Metastases
in vitro diagnosis of axillary lymph node metastases in breast cancer by spectrum analysis of radio frequency echo signals (Tateishi), 1151
in vitro investigation of lymph node metastasis of colorectal cancer using ultrasonic spectral parameters (Noritomi), 235
quantitative ultrasonic analysis of liver metastases (Huisman), 67
ultrasonographic evaluation of small cervical lymph nodes in head and neck cancer (Yoshida), 621

Metreweli, C., see Chan, S.-T.
Metreweli, C., see Ying, M.
Metter, E. J., see Nagai, Y.
Meves, S., see Postert, T.
Michel, E. and Zernikow, B.: Gosling's Doppler pulsatility index revisited, 597

Microbubbles
advantages of subharmonic over second harmonic backscatter for contrast-to-tissue echo enhancement (Shankar), 395
artificial cavitation nuclei significantly enhance acoustically induced cell transfection (Greenleaf), 587
effect of acoustic cavitation on platelets in the presence of an echo-contrast agent (Everbach), 129
diagnosis and monitoring of middle cerebral artery occlusion with contrast-enhanced transcranial color-coded real-time sonography in patients with inadequate acoustic bone windows (Postert), 333

dissolution of multicomponent microbubbles in the bloodstream: 1. Theory (Kabalnov), 739
dissolution of multicomponent microbubbles in the bloodstream: 2. Experiment (Kabalnov), 751
enhancement of ultrasonically-induced hemolysis by perfluorocarbon-based compared to air-based echo-contrast agents (Miller), 285
experimental study of stability of a contrast agent in an ultrasound field (Wu), 257
imaging and spectrum analysis of contrast agents in the *in vivo* rabbit eye using very-high-frequency ultrasound (Deng), 383
measurements of the nonlinearity parameter B/A of contrast agents (Wu), 153
standard properties of ultrasound contrast agents (Bouzakaz), 469
temperature rise generated by ultrasound in the presence of contrast agent (Wu), 267

Microemboli
the narrow band hypothesis: an interesting approach for high-intensity transient signals (HITS) detection (Roy), 375

Micronuclei
artificial cavitation nuclei significantly enhance acoustically induced cell transfection (Greenleaf), 587

Microscanning
40-MHz echocardiography scanner for cardiovascular assessment of mouse embryos (Aristizábal), 1407
acoustic properties of atherosclerosis of human aorta obtained with high-frequency ultrasound (Saijo), 1061
an investigation of possible effects of high-frequency ultrasound on cellular integrity of cultured fibroblasts (Chandraratna), 911
evaluation of acoustic properties of the live human smooth-muscle cell using scanning acoustic microscopy (Kinoshita), 1397
ultrasonic mapping of the microvasculature: signal alignment (Zagar), 809

Microvasculature
ultrasonic mapping of the microvasculature: signal alignment (Zagar), 809

Microwave therapy
ultrasound imaging of thermal therapy in *in vitro* liver (Gertner), 1023

Miller, D. L. and Gies, R. A.: enhancement of ultrasonically-induced hemolysis by perfluorocarbon-based compared to air-based echo-contrast agents, 285
Miller, D. L. and Gies, R. A.: gas-body-based contrast agent enhances vascular bioeffects of 1.09 MHz ultrasound on mouse intestine, 1201
Miller, D. L. and Gies, R. A.: the interaction of ultrasonic heating and cavitation in vascular bioeffects on mouse intestine, 123
Miller, H. I., see Alter, A.
Miller, M. W., see Doida, Y.
Minematsu, K., see Kimura, K.
Mizushige, K., see Kinoshita, A.
Moll, F. L., see Montauban van Swijndregt, A. D.
Molthen, R. C., Narayanan, V. M., Shankar, P. M., Reid, J. M., Genis, V.,

Forsberg, F., Halpern, E. J. and Goldberg, B. B.: using phase information in ultrasonic backscatter for *in vivo* liver analysis, 79
Molthen, R. C., Shankar, P. M., Reid, J. M., Forsberg, F., Halpern, E. J., Piccoli, C. W. and Goldberg, B. B.: comparison of the Rayleigh and K-distribution models using *in vivo* breast and liver tissue, 93

Monochorionicity
fetal biometry and outcome in monochorionic vs. dichorionic twin pregnancies; a retrospective cross-sectional matched-control study (Snijder), 197
Montauban van Swijndregt, A. D., Elbers, H. R. J., Moll, F. L., de Letter, J. and Ackerstaff, R. G. A.: ultrasonographic characterization of carotid plaques, 489
Montauban van Swijndregt, A. D., see de Groot, E.
Montenegro, N., see Bernardino, F.
Montrésor S., see Roy, E.
Moran, C. M., Anderson, T., Sboros, V., Sutherland, G. R., Wright, R. and McDicken, W. N.: quantification of the enhanced backscatter phenomenon from an intravenous and an intra-arterial contrast agent, 871
Moskalik, A. P., see Carson, P. L.

Motion detection
experimental verification of the correlation behavior of analytic ultrasound radiofrequency signals received from moving structures (Ledoux), 1383
multilevel and motion model-based ultrasonic speckle tracking algorithms (Yeung), 427
magnetic resonance imaging of ultrasonic fields (Walker), 137

Mouse
40-MHz echocardiography scanner for cardiovascular assessment of mouse embryos (Aristizábal), 1407
an investigation of possible effects of high-frequency ultrasound on cellular integrity of cultured fibroblasts (Chandraratna), 911
the interaction of ultrasonic heating and cavitation in vascular bioeffects on mouse intestine (Miller), 123

Movement
multilevel and motion model-based ultrasonic speckle tracking algorithms (Yeung), 427
respiratory ultrasonography of human parasternal intercostal muscle *in vivo* (Cala), 313

MRA
echo contrast-enhanced three-dimensional power Doppler of intracranial arteries (Postert), 953

MRI imaging
elastographic imaging of thermal lesions in soft tissue: a preliminary study *in vitro* (Stafford), 1449
in vitro measurement of kidney size: comparison of ultrasonography and MRI (Bakker), 683
magnetic resonance imaging of ultrasonic fields (Walker), 137
shear wave elasticity imaging: a new ultrasonic technology of medical diagnostics (Sarvazyan), 1419

Muscles
multilevel and motion model-based ultrasonic speckle tracking algorithms (Yeung), 427

Mutation
sonochemicals increase the mutation frequency of V79 cells *in vitro* (Doida), 1209

Myocardial infarction
ultrasonic tissue characterization for coronary care unit patients with acute myocardial infarction (Lin), 187
ultrasonic tissue characterization in predicting residual ischemia and myocardial viability for patients with acute myocardial infarction (Lin), 1107

Myocardium
color Doppler imaging of the myocardium: current status and potential clinical applications (Ofili), 177
improved quantification of myocardial mass by three-dimensional echocardiography using a deposit contrast agent (Kasprzak), 647
ultrasonic tissue characterization for coronary care unit patients with acute myocardial infarction (Lin), 187
ultrasonic tissue characterization in predicting residual ischemia and myocardial viability for patients with acute myocardial infarction (Lin), 1107

N

Nagai, Y., Kemper, M. K., Earley, C. J. and Metter, E. J.: blood-flow velocities and their relationships in carotid and middle cerebral arteries, 1131
Nanda, N. C., see Ofili, E. O.
Narang, Y., see Anthony, P.
Narayanan, V. M., see Molthen, R. C.
Nassiri, D. K., see Ramnarine, K. V.
Nattakom, S., see Carson, P. L.
Naya, Y., Kojima, M., Honjyo, H., Ochiai, A., Ukimara, O. and Watanabe, H.: intraobserver and interobserver variance in the measurement of ultrasound-estimated bladder weight, 771
Naylor, A. R., see Smith, J. L.
Nelson, T. R. and Pretorius, D. H.: three-dimensional ultrasound imaging, 1243

Neoplasms
contrast-enhanced sonography of tumor neovascularity in a rabbit model (Brown), 495

Neovascularity
contrast-enhanced sonography of tumor neovascularity in a rabbit model (Brown), 495

Netter, P., see Chérin, E.

Neural effects
focused ultrasound modifications of neural circuit activity in a mammalian brain (Bachtold), 557

Neurosurgery
limitations for three-dimensional ultrasound imaging through a bore-hold trepanation (Suhm), 663

Newhouse, V. L., see Shankar, P. M.
Newhouse, V. L., see Zheng, W.
Nitta, S., see Saijo, Y.

Non-linear parameter
measurements of the nonlinearity parameter B/A of contrast agents (Wu), 153

Non-Rayleigh
comparison of the Rayleigh and K-distribution models using *in vivo* breast and liver tissue (Molthen), 93

Noritomi, T., Machi, J., Feleppa, E. J., Yanagihara, E. and Shirouzu, K.: *in vitro* investigation of lymph node metastasis of colorectal cancer using ultrasonic spectral parameters, 235
Noritomi, T., see Tateishi, T.
Normolle, D., see Carson, P. L.
Nosir, Y. F. M., see Kasprzak, J. D.

NPL
the NPL Doppler fetal heart beat detector test facility (Bond), 443

Nudelman, S. P., see Hall, A. F.

O

O'Brien, S. P., see Lee, D. J.
Obladen, M., see Kampmann, W.

Observer variability
intra- and inter-observer variability and reliability of prostate volume measurement via two-dimensional and three-dimensional ultrasound imaging (Tong), 673
intraobserver and interobserver variance in the measurement of ultrasound-estimated bladder weight (Naya), 771

Ochiai, A., see Naya, Y.
Ødegaard, S., see Gilja, O. H.
Ofili, E. O. and Nanda, N. C.: color Doppler imaging of the myocardium: current status and potential clinical applications, 177
Ogata, J., see Kimura, K.
Oishi, R., see Tateishi, T.
Okawai, H., see Saijo, Y.
Olafsson, S., see Gilja, O. H.
Olofsson, P.-A., see Gudmundsson, S.
Olree, M., see Bakker, J.
Ophir, J., see Kallel, F.
Ophir, J., see Konofagou, E.
Ophir, J., see Stafford, R. J.
Ophir, J., see Varghese, T.

Osteoarthritis
evaluation of acoustical parameter sensitivity to age-related and osteoarthritic changes in articular cartilage using 50-MHZ ultrasound (Chérin), 341

Ostwald coefficient
dissolution of multicomponent microbubbles in the bloodstream: 1. Theory (Kabalnov), 739
dissolution of multicomponent microbubbles in the bloodstream: 2. Experiment (Kabalnov), 751

Otto, S., see Kabalnov, A.

Ovary
semiautomated segmentation of ovarian follicular ultrasound images using a knowledge-based algorithm (Sarty), 27

P

Pan, L., Zan, L. and Foster, F. S.: ultrasonic and viscoelastic properties of skin under transverse mechanical stress *in vitro*, 995
Pardi, G., see Pennati, G.
Parker, K. J., Fu, D., Graceswki, S. M., Yeung, F. and Levinson, S. F.: vibration sonoelasticity and the detectability of lesions, 1437
Parker, K. J., see Alam, S. K.
Parker, K.J., see Yeung, F.
Pasterkamp, G., see de Korte, C. L.
Patat, F., see Diridollou, S.
Pellerin, D., Berdeaux, A, Cohen, L., Giudicelli, J.-F., Witchitz, S. and Veyrat, C.: pre-ejectional left ventricular wall motions studied on conscious dogs using Doppler myocardial imaging: relationships with indices of left ventricular function, 1271
Pelura, T., see Kabalnov, A.
Pennati, G., Bellotti, M., Ferrazzi, E., Bozzo, M., Pardi, G. and Fumero, R.: blood flow through the ductus venosus in human fetus: calculation using Doppler velocimetry and computational findings, 477

Performance
3-D sonographic volume measurement of the cerebral ventricular system: *in vitro* validation (Kampmann), 1169
a new method for measuring the effective radiating area of physiotherapy treatment heads (Zeqiri), 761
a simple and accurate formula for the sound velocity in water (Lubbers), 1065
analysis of linear, area and volume distortion in 3D ultrasound imaging (Tong), 355
in vitro evaluation of three-dimensional ultrasonography based on magnetic scanhead tracking (Gilja), 1161
rapid calibration for 3-D freehand ultrasound (Prager), 855
the NPL Doppler fetal heart beat detector test facility (Bond), 443
validation of a new blood-mimicking fluid for use in Doppler flow test objects (Ramnarine), 451

Perfusion
3-D colour Doppler image quantification of breast masses (Carson), 945
color Doppler imaging of the myocardium: current status and potential clinical applications (Ofili), 177
factors affecting color Doppler energy ultrasound recordings in an in-vitro model (Gudmundsson), 899
ultrasonic mapping of the microvasculature: signal alignment (Zagar), 809

Peripheral volume flow
lower extremity volumetric arterial blood flow in normal subjects (Holland), 1079

Perkins, A. C.: ultrasound contrast agents, 307

Permeability
defects generated in human stratum corneum specimens by ultrasound (Wu), 705

Petechiae
gas-body-based contrast agent enhances vascular bioeffects of 1.09 MHz ultrasound on mouse intestine (Miller), 1201
the interaction of ultrasonic heating and cavitation in vascular bioeffects on mouse intestine (Miller), 123

Peters, B., see Kabalnov, A.
Pfundtner, N., see Postert, T.

Phantom
3-D sonographic volume measurement of the cerebral ventricular system: *in vitro* validation (Kampmann), 1169
a noninvasive method to estimate pulse wave velocity in arteries locally by means of ultrasound (Brands), 1325
a simple and accurate formula for the sound velocity in water (Lubbers), 1065
an acoustic injection test object for colour flow imaging systems (Li), 161
analysis of linear, area and volume distortion in 3D ultrasound imaging (Tong), 355
automatic registration of 3-D ultrasound images (Rohling), 841
blood flow imaging and volume flow quantitation with intravascular ultrasound (Li), 203
factors affecting color Doppler energy ultrasound recordings in an in-vitro model (Gudmundsson), 899
liquid or solid ultrasonically tissue-mimicking materials with very low scatter (Madsen), 535
quantification of sonographic echogenicity with grey-level histogram width: a clinical tissue characterization (Maeda), 225
quantification of the enhanced backscatter phenomenon from an intravenous and an intra-arterial contrast agent (Moran), 871
rapid calibration for 3-D freehand ultrasound (Prager), 855
using phase information in ultrasonic backscatter for *in vivo* liver analysis (Molthen), 79
validation of displacement measurements obtained from ultrasonic images during indentation testing (Kawchuk), 105

Phase analysis
using phase information in ultrasonic backscatter for *in vivo* liver analysis (Molthen), 79

Physiotherapy
a new method for measuring the effective radiating area of physiotherapy treatment heads (Zeqiri), 761

PI
color Doppler ultrasound pulsatile flow signals of thoracic lesions: comparison of lung cancers and benign lesions (Hsu), 1087

Gosling's Doppler pulsatility index revisited (Michel), 597
portal vein pulsatility ratio provides a measure of right heart function in chronic heart failure (Rengo), 327

Piccoli, C. W., see Molthen, R. C.
Pierson, R. A., see Sarty, G. E.

Pigs
hemostasis of punctured blood vessels using high-intensity focused ultrasound (Vaezy), 903
in vivo pressure measurements of lithotripsy shock waves in pigs (Cleveland), 293
sonographic observations of the gastroduodenal junction in neonatal piglets (Wright), 1337

Pirhonen, J., see Gudmundsson, S.

Placenta
fetal biometry and outcome in monochorionic vs. dichorionic twin pregnancies; a retrospective cross-sectional matched-control study (Snijder), 197
quantification of sonographic echogenicity with grey-level histogram width: a clinical tissue characterization (Maeda), 225

Placental weight
fetal biometry and outcome in monochorionic vs. dichorionic twin pregnancies; a retrospective cross-sectional matched-control study (Snijder), 197

Plaque
determination of carotid plaque risk by ultrasonic tissue characterization (Lee), 1291
influence of ECG-triggered data acquisition on reliability for carotid plaque volume measurements with a magnetic sensor three-dimensional ultrasound system (Delcker), 601
intravascular ultrasound elastography in human arteries: initial experience *in vitro* (de Korte), 401
ultrasonographic characterization of carotid plaques (Montauban van Swijndregt), 489

Plaque volume
influence of ECG-triggered data acquisition on reliability for carotid plaque volume measurements with a magnetic sensor three-dimensional ultrasound system (Delcker), 601

Platelets
effect of acoustic cavitation on platelets in the presence of an echo-contrast agent (Everbach), 129

Plewes, D. B., see Walker, C. L.
Popescu, O., see Klötzsch, C.

Portal vein
estimation of the human liver volume and configuration using three-dimensional ultrasonography: effect of a high-caloric liquid meal (Hausken), 1357
improved investigation of portal-hepatic veins by echo-enhanced Doppler sonography (Fischer), 1345

portal vein pulsatility ratio provides a measure of right heart function in chronic heart failure (Rengo), 327

Position sensing
automatic registration of 3-D ultrasound images (Rohling), 841
rapid calibration for 3-D freehand ultrasound (Prager), 855
vein graft surveillance with scanhead tracking duplex ultrasound imaging: a preliminary report (Jong), 1313

Post, E. J., see Wright, A. B.
Postert, T., Braun, B., Federlein, J., Przuntek, H., Köster, O. and Büttner, T.: diagnosis and monitoring of middle cerebral artery occlusion with contrast-enhanced transcranial color-coded real-time sonography in patients with inadequate acoustic bone windows, 333
Postert, T., Braun, B., Pfundtner, N., Sprengelmeyer, R., Meves, S., Przuntek, H. and Büttner, T.: echo contrast-enhanced three-dimensional power Doppler of intracranial arteries, 953

Power measurement
a new method for measuring the effective radiating area of physiotherapy treatment heads (Zeqiri), 761

Power spectrum analysis
in vitro investigation of lymph node metastasis of colorectal cancer using ultrasonic spectral parameters (Noritomi), 235

Prager, R. W., Rohling, R. N., Gee, A. H. and Berman, L.: rapid calibration for 3-D freehand ultrasound, 855
Prat, F., see Arefiev, A.
Prat, F., see Lafon, C.

Pressure
acoustic performance and clinical use of a fibreoptic hydrophone (Coleman), 143
demonstration of potential noninvasive ultrasound brain therapy through an intact skull (Hynynen), 275
enhancement of ultrasonically-induced hemolysis by perfluorocarbon-based compared to air-based echo-contrast agents (Miller), 285
experimental study of stability of a contrast agent in an ultrasound field (Wu), 257
in vivo pressure measurements of lithotripsy shock waves in pigs (Cleveland), 293
magnetic resonance imaging of ultrasonic fields (Walker), 137

Pressure distribution
demonstration of potential noninvasive ultrasound brain therapy through an intact skull (Hynynen), 275
in vivo pressure measurements of lithotripsy shock waves in pigs (Cleveland), 293

Preston, R. C., see Bond, A. D.
Pretorius, D. H., see Nelson, T. R.
Price, L. R., see Bachtold, M. R.
Price, R. E., see Stafford, R. J.
Primozich, J. F., see Jong, J.-M.

Prostate
elastographic imaging of low-contrast elastic modulus distributions in tissue (Kallel), 409
intra- and inter-observer variability and reliability of prostate volume measurement via two-dimensional and three-dimensional ultrasound imaging (Tong), 673

Przuntek, H., see Postert, T.

Pulse wave velocity
a noninvasive method to estimate pulse wave velocity in arteries locally by means of ultrasound (Brands), 1325

PVDF hydrophone
in vivo pressure measurements of lithotripsy shock waves in pigs (Cleveland), 293

Q

QA
3-D sonographic volume measurement of the cerebral ventricular system: *in vitro* validation (Kampmann), 1169
a new method for measuring the effective radiating area of physiotherapy treatment heads (Zeqiri), 761
a simple and accurate formula for the sound velocity in water (Lubbers), 1065
analysis of linear, area and volume distortion in 3D ultrasound imaging (Tong), 355
in vitro evaluation of three-dimensional ultrasonography based on magnetic scanhead tracking (Gilja), 1161
rapid calibration for 3-D freehand ultrasound (Prager), 855
the NPL Doppler fetal heart beat detector test facility (Bond), 443
validation of a new blood-mimicking fluid for use in Doppler flow test objects (Ramnarine), 451

Qin, Z., Durand, L.-G. and Cloutier, G.: Kinetics of the "Black Hole" phenomenon in ultrasound backscattering measurements with red blood cell aggregation, 245
Qin, Z., Durand, L.-G., Allard, L. and Cloutier, G.: effects of a sudden flow reduction on red blood cell rouleau formation and orientation using RF backscattered power, 503
Quedens-Case, C., see Brown, J. M.

R

Rabbit
contrast-enhanced sonography of tumor neovascularity in a rabbit model (Brown), 495
imaging and spectrum analysis of contrast agents in the *in vivo* rabbit eye using very-high-frequency ultrasound (Deng), 383
ultrasonic and viscoelastic properties of skin under transverse mechanical stress *in vitro* (Pan), 995

Rabbit eye
imaging and spectrum analysis of contrast agents in the *in vivo* rabbit eye using very-high-frequency ultrasound (Deng), 383

Rak, R., see Fischer, G.
Ramnarine, K. V., Nassiri, D. K., Hoskins, P. R. and Lubbers, J.: validation of a new blood-mimicking fluid for use in Doppler flow test objects, 451
Ramnarine, K. V., Nassiri, D. K., McCarthy, A. and Brown, N. A.: effects of pulsed ultrasound in embryonic development: an *in vitro* study, 575
Raninen, R. O.: ultrasound imaging for arterial wall thickness measurement: an *in vitro* study with stereomicroscopic correlation, 833
Rasmussen, J. G., see Vogt, K. C.

Rat
application of low-intensity ultrasound to growing bone in rats (Spadaro), 567
dynamic behavior of bubbles during extracorporeal shock-wave lithotripsy (Kodama), 723
effects of pulsed ultrasound on embryonic development: an *in vitro* study (Ramnarine), 575
focused ultrasound modifications of neural circuit activity in a mammalian brain (Bachtold), 557

Rawool, N. M., see Forsberg, F.

Rayleigh
comparison of the Rayleigh and K-distribution models using *in vivo* breast and liver tissue (Molthen), 93

Rayleigh-Plesset
acoustic modeling of shell-encapsulated gas bubbles (Frinking), 523

Red blood cell
effects of a sudden flow reduction on red blood cell rouleau formation and orientation using RF backscattered power (Qin), 503
extracorporeal shock waves act by shock wave-gas bubble interaction (Delius), 1055
in situ measurements of Doppler power vs. flow turbulence intensity in red cell suspensions (Wu), 1009

Red blood cell aggregation
effects of a sudden flow reduction on red blood cell rouleau formation and orientation using RF backscattered power (Qin), 503

Reflection coefficient
evaluation of acoustical parameter sensitivity to age-related and osteoarthritic changes in articular cartilage using 50-MHZ ultrasound (Chérin), 341

Registration
automatic registration of 3-D ultrasound images (Rohling), 841
rapid calibration for 3-D freehand ultrasound (Prager), 855

Regurgitation
aliasing-tolerant color Doppler quantification of regurgitant jets (Stewart), 881

Reiber, J. H. C., see van der Lugt, A.
Reid, J. M., see Molthen, R. C.
Reines, F., see Bachtold, M. R.

Relative echogenicity
the value of thyroid parenchymal echogenicity as an indicator of pathology using the sternomastoid muscle for comparison (Ying), 1097

Reneman, R. S., see Brands, P. J.
Reneman, R. S., see Willekes, C.
Rengo, C., Brevetti, G., Sorrentino, G., D'Amato, T., Imparato, M., Vitale, D. F., Acanfora, D. and Rengo, F.: portal vein pulsatility ratio provides a measure of right heart function in chronic heart failure, 327
Rengo, F., see Rengo, C.

Reperfusion
ultrasonic tissue characterization for coronary care unit patients with acute myocardial infarction (Lin), 187

Reproducibility
analysis of linear, area and volume distortion in 3D ultrasound imaging (Tong), 355
artifacts in intravascular ultrasound imaging during coronary artery stent implantation (Finet), 793
automated intima-media thickness: The Los Angeles Atherosclerosis Study (Dwyer), 981
in vitro evaluation of three-dimensional ultrasonography based on magnetic scanhead tracking (Gilja), 1161
in vitro measurement of kidney size: comparison of ultrasonography and MRI (Bakker), 683
influence of ECG-triggered data acquisition on reliability for carotid plaque volume measurements with a magnetic sensor three-dimensional ultrasound system (Delcker), 601
intra- and inter-observer variability and reliability of prostate volume measurement via two-dimensional and three-dimensional ultrasound imaging (Tong), 673
intraobserver and interobserver variance in the measurement of ultrasound-estimated bladder weight (Naya), 771
SieScape™: a new sonographic dimension with fictive images (Kröger), 1125
the NPL Doppler fetal heart beat detector test facility (Bond), 443
ultrasound imaging for arterial wall thickness measurement: an *in vitro* study with stereomicroscopic correlation (Raninen), 833
variance components analysis of carotid and femoral intima-media thickness measurements (de Groot), 825

Resistance Index
analysis of blood flow in adnexal tumors by using color Doppler imaging and pulsed spectral analysis (Takac), 1137
color Doppler sonography of normal breasts: detectability of arterial blood vessels and typical flow patterns (Rettenbacher), 1307
color Doppler ultrasound pulsatile flow signals of thoracic lesions: comparison of lung cancers and benign lesions (Hsu), 1087

Respiratory muscles
respiratory ultrasonography of human parasternal intercostal muscle *in vivo* (Cala), 313

Rettenbacher, T., Hollerweger, A., Macheiner, P. and Gritzmann, N.: color Doppler sonography of normal breasts: detectability of arterial blood vessels and typical flow patterns, 1307

Reynolds, J., see Kabalnov, A.

RF analysis
a new elastographic method for estimation and imaging of lateral displacements, lateral strains, corrected axial strains and Poisson's ratios in tissues (Konofagou), 1183
a noninvasive method to estimate pulse wave velocity in arteries locally by means of ultrasound (Brands), 1325
blood flow imaging and volume flow quantitation with intravascular ultrasound (Li), 203
effects of a sudden flow reduction on red blood cell rouleau formation and orientation using RF backscattered power (Qin), 503
evaluation of acoustical parameter sensitivity to age-related and osteoarthritic changes in articular cartilage using 50-MHZ ultrasound (Chérin), 341
experimental verification of the correlation behavior of analytic ultrasound radiofrequency signals received from moving structures (Ledoux), 1383
in vitro diagnosis of axillary lymph node metastases in breast cancer by spectrum analysis of radio frequency echo signals (Tateishi), 1151

Right heart function
portal vein pulsatility ratio provides a measure of right heart function in chronic heart failure (Rengo), 327

Rinaldi, P. C., see Bachtold, M. R.
Rivens, I. H., see Meaney, P. M.
Roberts, A. B., see Lee, D. J.
Rochester, D. F., see Cala, S. J.
Roelandt, J. R. T. C., see Bruining, N.
Roelandt, J. R. T.C., see Kasprzak, J. D.
Rohling, R. N., Gee, A. H. and Berman, L.: automatic registration of 3-D ultrasound images, 841
Rohling, R. N., see Prager, R. W.
Rosenbusch, G. J. E., see Huisman, H. J.
Rosenschein, U., see Alter, A.
Roubidoux, M. A., see Carson, P. L.

Rouleau
effects of a sudden flow reduction on red blood cell rouleau formation and orientation using RF backscattered power (Qin), 503

Roy, E., Abraham, P., Montrésor, S., Baudry, M. and Saumet, J.-L.: the narrow band hypothesis: an interesting approach for high-intensity transient signals (HITS) detection, 375
Roy, R., see Forsberg, F.
Rozenszajn, L. A., see Alter, A.
Rubin, J. M., see Carson, P. L.
Rudenko, O. V., see Sarvazyan, A. P.
Rudofsky, G., see Kröger, K.

S

Sackmann, M., see Fischer, G.

Safety
a new method for measuring the effective radiating area of physiotherapy treatment heads (Zeqiri), 761

effect of acoustic cavitation on platelets in the presence of an echo-contrast agent (Everbach), 129
demonstration of potential noninvasive ultrasound brain therapy through an intact skull (Hynynen), 275
effects of pulsed ultrasound on embryonic development: an *in vitro* study (Ramnarine), 575
enhancement of ultrasonically-induced hemolysis by perfluorocarbon-based compared to air-based echo-contrast agents (Miller), 285
in vivo heating of the guinea-pig fetal brain by pulsed ultrasound and estimates of thermal index (Horder), 1467
temperature rise generated by ultrasound in the presence of contrast agent (Wu), 267
treatment of implanted liver tumors with focused ultrasound (Chen), 1475
ultrasound-induced temperature increase in guinea-pig fetal brain *in utero*: third-trimester gestation (Horder), 1501

Saïed, A., see Chérin, E.
Saïed, A., see Lefebvre, F.
Saijo, Y., Sasaki, H., Okawai, H., Nitta, S. and Tanaka, M.: acoustic properties of atherosclerosis of human aorta obtained with high-frequency ultrasound, 1061
Sakamoto, S., see Kinoshita, A.
Salles-Cunha, S., see Fowlkes, J. B.
Saluja, A., see Fowlkes, J. B.
Sarkar, G., see Greenleaf, W. J.
Sarty, G. E., Liang, W., Sonka, M. and Pierson, R. A.: semiautomated segmentation of ovarian follicular ultrasound images using a knowledge-based algorithm, 27
Sarvazyan, A. P., Rudenko, O. V., Swanson, S. D., Fowlkes, J. B. and Emelianov, S. Y.: shear wave elasticity imaging: a new ultrasonic technology of medical diagnostics, 1419
Sasaki, H., see Saijo, Y.
Saumet, J.-L., see Roy, E.
Saunders, J. E., see Coleman, A. J.
Sboros, V., see Moran, C. M.

Scanhead tracking
vein graft surveillance with scanhead tracking duplex ultrasound imaging: a preliminary report (Jong), 1313

Scanning Acoustic Microscope
acoustic properties of atherosclerosis of human aorta obtained with high-frequency ultrasound (Saijo), 1061
evaluation of acoustic properties of the live human smooth-muscle cell using scanning acoustic microscopy (Kinoshita), 1397
evaluation of acoustical parameter sensitivity to age-related and osteoarthritic changes in articular cartilage using 50-MHZ ultrasound (Chérin), 341

Schöning, M. and Hartig, B.: the development of hemodynamics in the extracranial carotid and vertebral arteries, 655

Schlieren
in situ measurements of Doppler power vs. flow turbulence intensity in red cell suspensions (Wu), 1009

Schmid, A., see Schmidt-Trucksäss, A.
Schmidt-Trucksäss, A., Grathwohl, D., Schmid, A., Boragk, R., Upmeier, C., Keul, J. and Huonker, M.: assessment of carotid wall motion and stiffness with tissue Doppler imaging, 639
Schroeder, T. V., see Vogt, K. C.
Schutt, E., see Kabalnov, A.
Scoutt, L. M., see Holland, C. K.

Second harmonic
onset delay of acoustic second harmonic backscatter from bubbles or microspheres (Zheng), 513

Segmentation
automatic three-dimensional reconstruction and characterization of articular cartilage from high-resolution ultrasound acquisitions (Lefebvre), 1369
evaluation of model-based processing algorithms for averaged transmitral spectral Doppler images (Hall), 55
quantitative ultrasonic analysis of liver metastases (Huisman), 67
reliability and reproducibility of automated contour analysis in intravascular ultrasound images of femoropopliteal arteries (van der Lugt), 43
semiautomated segmentation of ovarian follicular ultrasound images using a knowledge-based algorithm (Sarty), 27
semiautomated ultrasonographic measurement of fetal nuchal translucency using a computer software tool (Bernardino), 51

Selzer, R. H., see Dwyer, J. H.

Semiautomated image analysis
semiautomated segmentation of ovarian follicular ultrasound images using a knowledge-based algorithm (Sarty), 27
semiautomated ultrasonographic measurement of fetal nuchal translucency using a computer software tool (Bernardino), 51
ultrasonic tissue characterization for coronary care unit patients with acute myocardial infarction (Lin), 187

Senda, S., see Kinoshita, A.
Senior, R.: advances in echo imaging using contrast enhancement, 1511

Sensitivity
the NPL Doppler fetal heart beat detector test facility (Bond), 443

Serruys, P. W. see Bruining, N.
Shankar, P. M., Krishna, P. D. and Newhouse, V. L.: advantages of subharmonic over second harmonic backscatter for contrast-to-tissue echo enhancement, 395
Shankar, P. M., see Molthen, R. C.

Shear wave imaging
shear wave elasticity imaging: a new ultrasonic technology of medical diagnostics (Sarvazyan), 1419

Sheehan, F. H., see Hausken, T.

Sheep
blood velocity profile in the ductus venosus inlet expressed by the mean/maximum velocity ratio (Kiserud), 1301

Sherar, M. D., see Gertner, M. R.

Shirouzu, K., see Noritomi, T.
Shirouzu, K., see Tateishi, T.

Shock waves
dynamic behavior of bubbles during extracorporeal shock-wave lithotripsy (Kodama), 1227 (Erratum),
dynamic behavior of bubbles during extracorporeal shock-wave lithotripsy (Kodama), 723
extracorporeal shock waves act by shock wave-gas bubble interaction (Delius), 1055
in vivo pressure measurements of lithotripsy shock waves in pigs (Cleveland), 293
innovative technology for tissue disruption by explosive-induced shock waves (Kodama), 1459
ultrasound-induced tissue ablation: studies on isolated, perfused porcine liver (Arefiev), 1033

Shotri, N., see Coleman, A. J.
Shung, K. K., see Wu, S. J.

Siescape
SieScape™: a new sonographic dimension with fictive images (Kröger), 1125

Sigel, B., see Lee, D. J.
Sigel, B.: a brief history of Doppler ultrasound in the diagnosis of peripheral vascular disease, 169

Signal alignment
ultrasonic mapping of the microvasculature: signal alignment (Zagar), 809

Sillesen, H., see Vogt, K. C.
Silverman, R. H., see Deng, C. X.
Simons, P. C. G., Bots, M. L., Algra, A., van Teeffelen, A. S. P. and van der Graaf, Y., for the SMART Study Group: effect of timing of blood pressure measurement in the assessment of arterial stiffness: The SMART Study, 1285

Skin
an *in vivo* method for measuring the mechanical properties of the skin using ultrasound (Diridollou), 215
ultrasonic and viscoelastic properties of skin under transverse mechanical stress *in vitro* (Pan), 995

Skovgaard, L. T., see Vogt, K. C.

Skull
demonstration of potential noninvasive ultrasound brain therapy through an intact skull (Hynynen), 275

Smith, J. L., Evans, D. H., Bell, P. R. F. and Naylor, A. R.: time domain analysis of embolic signals can be used in place of high-resolution Wigner analysis when classifying gaseous and particulate emboli, 989
Smith, N. B. and Hynynen, K.: the feasibility of using focused ultrasound for transmyocardial revascularization, 1045
Snijder, M. J. and Wladimiroff, J. W.: fetal biometry and outcome in monochorionic vs. dichorionic twin pregnancies; a retrospective cross-sectional matched-control study, 197

Sonka, M., see Sarty, G. E.

Sonochemicals
sonochemicals increase the mutation frequency of V79 cells *in vitro* (Doida), 1209

Sorrentino, G., see Rengo, C.

Sound speed
a simple and accurate formula for the sound velocity in water (Lubbers), 1065
acoustic properties of atherosclerosis of human aorta obtained with high-frequency ultrasound (Saijo), 1061
evaluation of acoustic properties of the live human smooth-muscle cell using scanning acoustic microscopy (Kinoshita), 1397
magnetic resonance imaging of ultrasonic fields (Walker), 137
ultrasonic and viscoelastic properties of skin under transverse mechanical stress *in vitro* (Pan), 995

Spadaro, J. A. and Albanese, S. A.: application of low-intensity ultrasound to growing bone in rats, 567

Spatial compounding
automatic registration of 3-D ultrasound images (Rohling), 841

Speckle tracking
multilevel and motion model-based ultrasonic speckle tracking algorithms (Yeung), 427

Spectral analysis
imaging and spectrum analysis of contrast agents in the *in vivo* rabbit eye using very-high-frequency ultrasound (Deng), 383
the narrow band hypothesis: an interesting approach for high-intensity transient signals (HITS) detection (Roy), 375

Splanchnic circulation
duodenal meal stimulation leads to coeliac artery vasoconstriction and superior mesenteric artery vasodilatation: an intra-abdominal ultrasound study (Geelkerken), 1351

Sprengelmeyer, R., see Postert, T.
Stafford, R. J., Kallel, F., Price, R. E., Cromeens, D. M., Krouskop, T. A., Hazle, J. D. and Ophir, J.: elastographic imaging of thermal lesions in soft tissue: a preliminary study *in vitro*, 1449

Standardization
a simple and accurate formula for the sound velocity in water (Lubbers), 1065
standard properties of ultrasound contrast agents (Bouzakaz), 469
the NPL Doppler fetal heart beat detector test facility (Bond), 443
validation of a new blood-mimicking fluid for use in Doppler flow test objects (Ramnarine), 451

STAR
standard properties of ultrasound contrast agents (Bouzakaz), 469

Starritt, H.: safety of diagnostic ultrasound, 1513

Stenosis
quantification of iliac artery stenoses: a methodological comparative study between intravascular ultrasound, arteriography and duplex scanning (Vogt), 963
vein graft surveillance with scanhead tracking duplex ultrasound imaging: a preliminary report (Jong), 1313

Stent
artifacts in intravascular ultrasound imaging during coronary artery stent implantation (Finet), 793
dynamic imaging of coronary stent structures: an ECG-gated three-dimensional intracoronary ultrasound study in humans (Bruining), 631

Sternomastoid muscle
the value of thyroid parenchymal echogenicity as an indicator of pathology using the sternomastoid muscle for comparison (Ying), 1097

Stewart, S. F. C.: aliasing-tolerant color Doppler quantification of regurgitant jets, 881

Stiffness
validation of displacement measurements obtained from ultrasonic images during indentation testing (Kawchuk), 105

Stomach
sonographic observations of the gastroduodenal junction in neonatal piglets (Wright), 1337

Strain
a new elastographic method for estimation and imaging of lateral displacements, lateral strains, corrected axial strains and Poisson's ratios in tissues (Konofagou), 1183
an analysis of elastographic contrast-to-noise ratio (Varghese), 915
an *in vivo* method for measuring the mechanical properties of the skin using ultrasound (Diridollou), 215
characterization of elastographic noise using the envelope of echo signals (Varghese), 543
elastographic imaging of low-contrast elastic modulus distributions in tissue (Kallel), 409
elastographic imaging of thermal lesions in soft tissue: a preliminary study *in vitro* (Stafford), 1449
intravascular ultrasound elastography in human arteries: initial experience *in vitro* (de Korte), 401
limits on the contrast of strain concentrations in elastography (Kallel), 1215

Strandness, D. E. Jr., see Jong, J.-M.

Streaming
hemostasis of punctured blood vessels using high-intensity focused ultrasound (Vaezy), 903

Stress
a new elastographic method for estimation and imaging of lateral displacements, lateral strains, corrected axial strains and Poisson's ratios in tissues (Konofagou), 1183

an *in vivo* method for measuring the mechanical properties of the skin using ultrasound (Diridollou), 215
limits on the contrast of strain concentrations in elastography (Kallel), 1215
ultrasonic and viscoelastic properties of skin under transverse mechanical stress *in vitro* (Pan), 995

Strieter, R. M., see Fowlkes, J. B.

Stroke
determination of carotid plaque risk by ultrasonic tissue characterization (Lee), 1291
oscillating thromboemboli within the extracranial internal carotid artery demonstrated by ultrasonography in patients with acute cardioembolic stroke (Kimura), 1121

Struijk, P. C., see Ursem, N. T. C.

Subharmonic imaging
advantages of subharmonic over second harmonic backscatter for contrast-to-tissue echo enhancement (Shankar), 395

Sudden infant death syndrome
sonographic observations of the gastroduodenal junction in neonatal piglets (Wright), 1337

Suhm, N., Dams, J., van Leyen, K., Lorenz, A. and Bendl, R.: limitations for three-dimensional ultrasound imaging through a bore-hold trepanation, 663
Sun, P., see Dwyer, J. H.

Surgery
demonstration of potential noninvasive ultrasound brain therapy through an intact skull (Hynynen), 275
elastographic imaging of thermal lesions in soft tissue: a preliminary study *in vitro* (Stafford), 1449
hemostasis of punctured blood vessels using high-intensity focused ultrasound (Vaezy), 903
history of intraoperative ultrasound (Makuuchi), 1229
treatment of implanted liver tumors with focused ultrasound (Chen), 1475
ultrasound-induced tissue ablation: studies on isolated, perfused porcine liver (Arefiev), 1033

Sutherland, G. R., see Moran, C. M.
Swami, V. K., see Lee, D. J.
Swanson, S. D., see Sarvazyan, A. P.

T

Takac, I.: analysis of blood flow in adnexal tumors by using color Doppler imaging and pulsed spectral analysis, 1137
Takayama, K., see Kodama, T.
Tanaka, M., see Saijo, Y.
Tateishi, T., Machi, J., Feleppa, E. J., Oishi, R., Jucha, J., Yanagihara, E., McCarthy, L. J., Noritomi, T. and Shirouzu, K.: in vitro diagnosis of axillary lymph node metastases in breast cancer by spectrum analysis of radio frequency echo signals, 1151
Tavakkoli, J., see Arefiev, A.

Taylor, K. J. W., see Brown, J. M.
Taylor, K. J. W., see Holland, C. K.

TCD
a new 1-MHz probe for transcranial Doppler sonography in patients with inadequate temporal bone windows (Klötzsch), 101
diagnosis and monitoring of middle cerebral artery occlusion with contrast-enhanced transcranial color-coded real-time sonography in patients with inadequate acoustic bone windows (Postert), 333
time domain analysis of embolic signals can be used in place of high-resolution Wigner analysis when classifying gaseous and particulate emboli (Smith), 989

Tegeler, C, see Delcker, A.

Temperature
a 3-D finite-element model for computation of temperature profiles and regions of thermal damage during focused ultrasound surgery exposures (Meaney), 1489
demonstration of potential noninvasive ultrasound brain therapy through an intact skull (Hynynen), 275
in vivo heating of the guinea-pig fetal brain by pulsed ultrasound and estimates of thermal index (Horder), 1467
temperature rise generated by ultrasound in the presence of contrast agent (Wu), 267
ultrasound-induced temperature increase in guinea-pig fetal brain *in utero*: third-trimester gestation (Horder), 1501
ultrasound-induced temperature increase in the guinea-pig fetal brain *in vitro* (Horder), 697

Temporal bone
a new 1-MHz probe for transcranial Doppler sonography in patients with inadequate temporal bone windows (Klötzsch), 101

Ten Cate, F. J., see Kasprzak, J. D.

Test object
3-D sonographic volume measurement of the cerebral ventricular system: *in vitro* validation (Kampmann), 1169
a noninvasive method to estimate pulse wave velocity in arteries locally by means of ultrasound (Brands), 1325
a simple and accurate formula for the sound velocity in water (Lubbers), 1065
an acoustic injection test object for colour flow imaging systems (Li), 161
analysis of linear, area and volume distortion in 3D ultrasound imaging (Tong), 355
automatic registration of 3-D ultrasound images (Rohling), 841
blood flow imaging and volume flow quantitation with intravascular ultrasound (Li), 203
factors affecting color Doppler energy ultrasound recordings in an in-vitro model (Gudmundsson), 899
liquid or solid ultrasonically tissue-mimicking materials with very low scatter (Madsen), 535
quantification of sonographic echogenicity with grey-level histogram width: a clinical tissue characterization (Maeda), 225

quantification of the enhanced backscatter phenomenon from an intravenous and an intra-arterial contrast agent (Moran), 871
rapid calibration for 3-D freehand ultrasound (Prager), 855
using phase information in ultrasonic backscatter for *in vivo* liver analysis (Molthen), 79
validation of displacement measurements obtained from ultrasonic images during indentation testing (Kawchuk), 105

Theillére, Y., see Lafon, C.

Therapy
a 3-D finite-element model for computation of temperature profiles and regions of thermal damage during focused ultrasound surgery exposures (Meaney), 1489
a new method for measuring the effective radiating area of physiotherapy treatment heads (Zeqiri), 761
application of low-intensity ultrasound to growing bone in rats (Spadaro), 567
artificial cavitation nuclei significantly enhance acoustically induced cell transfection (Greenleaf), 587
demonstration of potential noninvasive ultrasound brain therapy through an intact skull (Hynynen), 275
design and preliminary results of an ultrasound applicator for interstitial thermal coagulation (Lafon), 113
hemostasis of punctured blood vessels using high-intensity focused ultrasound (Vaezy), 903
the feasibility of using focused ultrasound for transmyocardial revascularization (Smith), 1045
treatment of implanted liver tumors with focused ultrasound (Chen), 1475
ultrasound inhibits the adhesion and migration of smooth muscle cells *in vitro* (Alter), 711
ultrasound-induced tissue ablation: studies on isolated, perfused porcine liver (Arefiev), 1033

Thermal effects
a 3-D finite-element model for computation of temperature profiles and regions of thermal damage during focused ultrasound surgery exposures (Meaney), 1489
demonstration of potential noninvasive ultrasound brain therapy through an intact skull (Hynynen), 275
design and preliminary results of an ultrasound applicator for interstitial thermal coagulation (Lafon), 113
elastographic imaging of thermal lesions in soft tissue: a preliminary study *in vitro* (Stafford), 1449
focused ultrasound modifications of neural circuit activity in a mammalian brain (Bachtold), 557
hemostasis of punctured blood vessels using high-intensity focused ultrasound (Vaezy), 903
high frequency ultrasound properties of multicellular spheroids during heating (Gertner), 461
in vivo heating of the guinea-pig fetal brain by pulsed ultrasound and estimates of thermal index (Horder), 1467
temperature rise generated by ultrasound in the presence of contrast agent (Wu), 267
ultrasound imaging of thermal therapy in *in vitro* liver (Gertner), 1023

ultrasound-induced temperature increase in guinea-pig fetal brain *in utero*: third-trimester gestation (Horder), 1501
ultrasound-induced temperature increase in the guinea-pig fetal brain *in vitro* (Horder), 697

Thermal Index
in vivo heating of the guinea-pig fetal brain by pulsed ultrasound and estimates of thermal index (Horder), 1467

Thermal therapy
high frequency ultrasound properties of multicellular spheroids during heating (Gertner), 461
ultrasound imaging of thermal therapy in *in vitro* liver (Gertner), 1023

Thickness
evaluation of acoustical parameter sensitivity to age-related and osteoarthritic changes in articular cartilage using 50-MHZ ultrasound (Chérin), 341

Thijssen, J. M., see Huisman, H. J.

Thoracic lesions
color Doppler ultrasound pulsatile flow signals of thoracic lesions: comparison of lung cancers and benign lesions (Hsu), 1087

Thromboendarterectomy
the use of intravascular ultrasound for intraoperative assessment during semiclosed thromboendarterectomy (Vogt), 21

Thrombosis
oscillating thromboemboli within the extracranial internal carotid artery demonstrated by ultrasonography in patients with acute cardioembolic stroke (Kimura), 1121
ultrasound echogenicity in experimental venous thrombosis (Fowlkes), 1175

Thyroid
alteration of thyroid blood flow during the normal menstrual cycle in healthy Chinese women (Chan), 15
the value of thyroid parenchymal echogenicity as an indicator of pathology using the sternomastoid muscle for comparison (Ying), 1097

Thyroiditis
the value of thyroid parenchymal echogenicity as an indicator of pathology using the sternomastoid muscle for comparison (Ying), 1097

Thyrotoxicosis
the value of thyroid parenchymal echogenicity as an indicator of pathology using the sternomastoid muscle for comparison (Ying), 1097

TIA
determination of carotid plaque risk by ultrasonic tissue characterization (Lee), 1291

Time domain processing
in vivo validation of the time domain velocity measurement technique of blood flow in human fetuses (Alcázar), 9

Tiptaf, R., see Coleman, A. J.

Tissue characterization
comparison of the Rayleigh and K-distribution models using *in vivo* breast and liver tissue (Molthen), 93
determination of carotid plaque risk by ultrasonic tissue characterization (Lee), 1291
evaluation of acoustic properties of the live human smooth-muscle cell using scanning acoustic microscopy (Kinoshita), 1397
high frequency ultrasound properties of multicellular spheroids during heating (Gertner), 461
in vitro diagnosis of axillary lymph node metastases in breast cancer by spectrum analysis of radio frequency echo signals (Tateishi), 1151
intravascular ultrasound elastography in human arteries: initial experience *in vitro* (de Korte), 401
quantitative ultrasonic analysis of liver metastases (Huisman), 67
shear wave elasticity imaging: a new ultrasonic technology of medical diagnostics (Sarvazyan), 1419
the value of thyroid parenchymal echogenicity as an indicator of pathology using the sternomastoid muscle for comparison (Ying), 1097
ultrasonic tissue characterization for coronary care unit patients with acute myocardial infarction (Lin), 187
ultrasonic tissue characterization in predicting residual ischemia and myocardial viability for patients with acute myocardial infarction (Lin), 1107
ultrasonographic characterization of carotid plaques (Montauban van Swijndregt), 489
using phase information in ultrasonic backscatter for *in vivo* liver analysis (Molthen), 79
validation of displacement measurements obtained from ultrasonic images during indentation testing (Kawchuk), 105

Tissue Doppler imaging
assessment of carotid wall motion and stiffness with tissue Doppler imaging (Schmidt-Trucksäss), 639

Tissue mimicking
liquid or solid ultrasonically tissue-mimicking materials with very low scatter (Madsen), 535

TOE
clinical transesophageal echocardiography - a problem-oriented approach (Wright), 307

Tohno, E., see Yoshida, H.
Tong, J., see Wu, J.
Tong, S., Cardinal, H. N., Downey, D. B. and Fenster, A.: analysis of linear, area and volume distortion in 3D ultrasound imaging, 355
Tong, S., Cardinal, H. N., McLoughlin, R. F., Downey, D. B. and Fenster, A.: intra- and inter-observer variability and reliability of prostate volume measurement via two-dimensional and three-dimensional ultrasound imaging, 673
Torzilli, G., see Makuuchi, M.

Transcranial imaging
diagnosis and monitoring of middle cerebral artery occlusion with contrast-enhanced transcranial color-coded real-time sonography in patients with inadequate acoustic bone windows (Postert), 333
echo contrast-enhanced three-dimensional power Doppler of intracranial arteries (Postert), 953

Transdermal drug delivery
defects generated in human stratum corneum specimens by ultrasound (Wu), 705

Transducer
a new 1-MHz probe for transcranial Doppler sonography in patients with inadequate temporal bone windows (Klötzsch), 101
an *in vivo* method for measuring the mechanical properties of the skin using ultrasound (Diridollou), 215
demonstration of potential noninvasive ultrasound brain therapy through an intact skull (Hynynen), 275
design and preliminary results of an ultrasound applicator for interstitial thermal coagulation (Lafon), 113

Transfection
artificial cavitation nuclei significantly enhance acoustically induced cell transfection (Greenleaf), 587

Transmitral spectral Doppler
evaluation of model-based processing algorithms for averaged transmitral spectral Doppler images (Hall), 55

Transmyocardial revascularisation
the feasibility of using focused ultrasound for transmyocardial revascularization (Smith), 1045

Transrectal
intra- and inter-observer variability and reliability of prostate volume measurement via two-dimensional and three-dimensional ultrasound imaging (Tong), 673

Tsunoda-Shimizu, H., see Yoshida, H.

Tumour detection
vibration sonoelastography and the detectability of lesions (Parker), 1437

Tumour flow
analysis of blood flow in adnexal tumors by using color Doppler imaging and pulsed spectral analysis (Takac), 1137

Turbulence
in situ measurements of Doppler power vs. flow turbulence intensity in red cell suspensions (Wu), 1009

Turnbull, D. H., see Aristizábal, O.

Twin pregnancy
fetal biometry and outcome in monochorionic vs. dichorionic twin pregnancies; a retrospective cross-sectional matched-control study (Snijder), 197

Twining, P.: atlas of ultrasound colour flow imaging, 1514

U

Uchino, M., see Kimura, K.
Ueberle, F., see Delius, M.
Ueno, E., see Yoshida, H.
Uenohara, H., see Kodama, T.
Ukimara, O., see Naya, Y.

Ultrasound field imaging
magnetic resonance imaging of ultrasonic fields (Walker), 137

Umbilical artery
in vivo validation of the time domain velocity measurement technique of blood flow in human fetuses (Alcázar), 9
umbilical artery waveform analysis based on maximum, mean and mode velocity in early human pregnancy (Ursem), 1

Upmeier, C., see Schmidt-Trucksäss, A.
Ursea, R., see Deng, C. X.
Ursem, N. T. C., Brinkman, H. J. F., Struijk, P. C., Hop, W. C. J., Kempski, M. H., Keller, B. B. and Wladimiroff, J. W.: umbilical artery waveform analysis based on maximum, mean and mode velocity in early human pregnancy, 1

US guidance
interventional ultrasound in Europe (Holm), 779

Utsu, M., see Maeda, K.

V

Vabre, V., see Diridollou, S.
Vaezy, S., Martin, R., Yaziji, H., Kaczkowski, P., Keilman, G., Carter, S., Caps, M., Chi, E. Y., Bailey, M. and Crum, L.: hemostasis of punctured blood vessels using high-intensity focused ultrasound, 903
Vaezy, S., see Hausken, T.
Vaillant, L., see Diridollou, S.
Valentin, L., see Gudmundsson, S.
van Bockel, J. H., see Geelkerken, R. H.
van der Graaf, Y., see Simons, P. C. G.
van der Lugt, A., Hartlooper, A., van Essen, J. A., Li, W., von Birgelen, C., Reiber, J. H. C. and Gussenhoven, E. J.: reliability and reproducibility of automated contour analysis in intravascular ultrasound images of femoropopliteal arteries, 43
van der Steen, A. F. W., see de Groot, E.
van der Steen, A. F. W., see de Korte, C. L.
van der Steen, A. F. W., see Li, W.
van der Steen, A. F. W.: intravascular ultrasound imaging in cronary artery disease, 1511
van Essen, J. A., see van der Lugt, A.
van Leyen, K., see Suhm, N.
van Meegen, J. R., see Kasprzak, J. D.
van Teeffelen, A. S. P., see Simons, P. C. G.

Varghese, T. and Ophir, J.: an analysis of elastographic contrast-to-noise ratio, 915
Varghese, T. and Ophir, J.: characterization of elastographic noise using the envelope of echo signals, 543

Vascular autoregulation
Gosling's Doppler pulsatility index revisited (Michel), 597

Vein graft
vein graft surveillance with scanhead tracking duplex ultrasound imaging: a preliminary report (Jong), 1313

Vella, G. J., see Horder, M. M.

Velocimetry
in vivo validation of the time domain velocity measurement technique of blood flow in human fetuses (Alcázar), 9
umbilical artery waveform analysis based on maximum, mean and mode velocity in early human pregnancy (Ursem), 1

Velocity distribution
blood flow through the ductus venosus in human fetus: calculation using Doppler velocimetry and computational findings (Pennati), 477

Velocity profile
blood velocity profile in the ductus venosus inlet expressed by the mean/maximum velocity ratio (Kiserud), 1301

Vertebral artery
the development of hemodynamics in the extracranial carotid and vertebral arteries (Schöning), 655

Veyrat, C., see Pellerin, D.

Viscerovascular reflex
bladder filling reduces femoral artery wall distension and strain: beware of a full bladder! (Willekes), 803

Viscoelasticity
ultrasonic and viscoelastic properties of skin under transverse mechanical stress *in vitro* (Pan), 995
vibration sonoelastography and the detectability of lesions (Parker), 1437

Vitale, D. F., see Rengo, C.
Vletter, W. B., see Kasprzak, J. D.
Vogel, M., see Kampmann, W.
Vogt, K. C., Rasmussen, J. G., Skovgaard, L. T., Just, S. and Schroeder, T. V.: quantification of iliac artery stenoses: a methodological comparative study between intravascular ultrasound, arteriography and duplex scanning
Vogt, K. C., Sillesen, H. and Schroeder, T. V.: the use of intravascular ultrasound for intraoperative assessment during semiclosed thromboendarterectomy, 21

Volume
3-D sonographic volume measurement of the cerebral ventricular system: *in vitro* validation (Kampmann), 1169

analysis of linear, area and volume distortion in 3D ultrasound imaging (Tong), 355
automatic registration of 3-D ultrasound images (Rohling), 841
improved quantification of myocardial mass by three-dimensional echocardiography using a deposit contrast agent (Kasprzak), 647
in vitro evaluation of three-dimensional ultrasonography based on magnetic scanhead tracking (Gilja), 1161
in vitro measurement of kidney size: comparison of ultrasonography and MRI (Bakker), 683
influence of ECG-triggered data acquisition on reliability for carotid plaque volume measurements with a magnetic sensor three-dimensional ultrasound system (Delcker), 601
intra- and inter-observer variability and reliability of prostate volume measurement via two-dimensional and three-dimensional ultrasound imaging (Tong), 673
rapid calibration for 3-D freehand ultrasound (Prager), 855

Volume flow
blood flow imaging and volume flow quantitation with intravascular ultrasound (Li), 203
lower extremity volumetric arterial blood flow in normal subjects (Holland), 1079

Volume imaging
three-dimensional ultrasound imaging (Nelson), 1243

von Birgelen, C., see Bruining, N.
von Birgelen, C., see van der Lugt, A.

W

Wada, K., see Kimura, K.
Wagener, D. J. Th., see Huisman, H. J.
Wakefield, T. W., see Fowlkes, J. B.
Walka, M. M., see Kampmann, W.
Walker, C. L., Foster, F. S. and Plewes, D. B.: magnetic resonance imaging of ultrasonic fields, 137

Wall motion
assessment of carotid wall motion and stiffness with tissue Doppler imaging (Schmidt-Trucksäss), 639

Warning
bladder filling reduces femoral artery wall distension and strain: beware of a full bladder! (Willekes), 803

Watanabe, H., see Naya, Y.

Water
a simple and accurate formula for the sound velocity in water (Lubbers), 1065

Watkin, K., see Cala, S. J.
Wear, K. A. and Garra, B. S.: assessment of bone density using ultrasonic backscatter, 689
Weers, J., see Kabalnov, A.
Weimann, L., see Wu, J.

Wells, P. N. T.: a note from the Editor-in-Chief, 607

WFUMB
World Federation for Ultrasound in Medicine and Biology Constitution, 931
Willekes, C., Hoogland, H. J., Hoeks, A. P. G. and Reneman, R. S.: bladder filling reduces femoral artery wall distension and strain: beware of a full bladder!, 803
Willigers, J. M., see Brands, P. J.
Willigers, J. M., see Ledoux, L. A. F.
Willis, L. R., see Cleveland, R. O.
Wilson, B. C., see Gertner, M. R.
Witchitz, S., see Pellerin, D.
Wladimiroff, J. W., see Snijder, M. J.
Wladimiroff, J. W., see Ursem, N. T. C.
Wood, A. K. W., see Horder, M. M.
Wood, A. K. W., see Wright, A. B.
World Federation for Ultrasound in Medicine and Biology Constitution, 931
Worthington, A. E., see Gertner, M. R.
Wright, A. B., McKelvey, G. M., Wood, A. K. W. and Post, E. J.: sonographic observations of the gastroduodenal junction in neonatal piglets, 1337
Wright, R. A.: clinical transesophageal echocardiography - a problem-oriented approach, 307
Wright, R., see Moran, C. M.
Wrobleski, S. K., see Fowlkes, J. B.
Wu, C.-C., see Lin, L.-C.
Wu, J. and Tong, J.: experimental study of stability of a contrast agent in an ultrasound field, 257
Wu, J. and Tong, J.: measurements of the nonlinearity parameter B/A of contrast agents, 153
Wu, J., Chappelow, J., Yang, J. and Weimann, L.: defects generated in human stratum corneum specimens by ultrasound, 705
Wu, J.: temperature rise generated by ultrasound in the presence of contrast agent, 267
Wu, S. J., Shung, K. K. and Brasseur, J. G.: *in situ* measurements of Doppler power vs. flow turbulence intensity in red cell suspensions, 1009

Y

Yamaguchi, T., see Kimura, K.
Yanagihara, E., see Noritomi, T.
Yanagihara, E., see Tateishi, T.
Yang, J., see Wu, J.
Yasaka, M., see Kimura, K.
Yaziji, H., see Vaezy, S.
Yeung, F., Levinson, S. F. and Parker, K.J.: multilevel and motion model-based ultrasonic speckle tracking algorithms, 427
Yeung, F., see Parker, K. J.
Ying, M., Brook, F., Ahuja, A. and Metreweli, C.: the value of thyroid parenchymal echogenicity as an indicator of pathology using the sternomastoid muscle for comparison, 1097
Yonemura, K., see Kimura, K.
Yoshida, H., Yusa, H., Ueno, E., Tohno, E. and Tsunoda-Shimizu, H.: ultrasonographic evaluation of small cervical lymph nodes in head and neck cancer, 621

Young's Modulus
elastographic imaging of low-contrast elastic modulus distributions in tissue (Kallel), 409
ultrasonic and viscoelastic properties of skin under transverse mechanical stress *in vitro* (Pan), 995

Yusa, H., see Yoshida, H.
Yvon, C., see Diridollou, S.

Z

Zagar, B. G., Fornaris, R. J. and Ferrara, K. W.: ultrasonic mapping of the microvasculature: signal alignment, 809
Zan, L., see Pan, L.
Zeqiri, B. and Hodnett, M.: a new method for measuring the effective radiating area of physiotherapy treatment heads, 761
Zernikow, B., see Michel, E.
Zheng, W. and Newhouse, V. L.: onset delay of acoustic second harmonic backscatter from bubbles or microspheres, 513
Zwijsen, J. H. M. J., see Geelkerken, R. H.
Zwinderman, A. H., see de Groot, E.